공학석사 학위논문

Statistical Analysis of Structural parameters for a Photobioreactor design

광생물반응기 설계를 위한 구조변수의 통계적 분석

2016 년 2 월

서울대학교 대학원

생태조경 · 지역시스템공학부 지역시스템공학전공

여 욱 현

Statistical Analysis of Structural parameters for a Photobioreactor design

광생물반응기 설계를 위한 구조변수의 통계적 분석

지도교수 이 인 복

이 논문을 공학석사 학위논문으로 제출함
2016 년 2 월

서울대학교 대학원
생태조경 · 지역시스템공학부 지역시스템공학전공
여 욱 현

여욱현의 공학석사 학위논문을 인준함
2016년 2 월

위 원 장 _____(인)

부위원장 _____(인)

위 원 _____(인)

Abstract

Korea showed a high dependence on imported energy amounting to approximately 95% in 2014 (KEEI, 2014). However, The high dependency on oil can be a threatening factor for the national economy and energy security according to the supply and demand status of crude oil, and it has been known that there is a possibility to exacerbate abnormal weather phenomena caused by global warming depending on the combination with carbon dioxide in the combustion process of most of carbon compounds. Therefore, The Korean government recently announced a plan to increases the proportion of new and renewable energy to up to 13.4% of the total amount of power until 2035, which was only 3.5% in 2013 (MOTIE, 2014).

The biomass among new and renewable energy produced in a year on earth is similar to all oil deposits, and there is no concern of this source becoming exhausted when using it properly. In particular, the bio-diesel fuel of biomass is a unique liquid fuel, and it can be utilized for large transport vehicles.

Microalgae, which is a third-generation biomass resource used to produce bio-diesel, contains a 1,000 times higher lipid content compared with different types of production resources in terms of the same culture area based on a rapid growth rate and has recently attracted attention. The microalgae, a single-cell organisms living in water and growing based on photosynthesis, uses sunlight, CO_2, nutrients (N, P), etc. in the culture process. Culture systems for microalgae are largely divided into two types: open and closed. The open system is simple to enlarge for commercial production, but it is difficult to maintain the optimal culture condition due to natural environmental conditions. The closed system (photobioreactor, PBR) allows for avoiding water losses and controlling culture environmental conditions artificially. It also allows for minimizing the inflow of contaminants and the loss of the carbon dioxide injected into the PBR. In particular, the PBR was known as a

feasible system in Korea in terms of narrow area of territory because it does not require too much area for installation.

In general, the enlargement for the PBR is essential to commercialize and to secure lots of energy resources. However, the production of microalgae was dramatically diminished by decreasing the light penetration rate in accordance with the capacity increase (mainly, the depth of the PBR). The production of microalgae can be increased by improving the light intensity and light homogeneity. That is, the PBRs with a suitable dimension can enhance the productivity by properly considering the flow characteristics inside the PBR caused by structural parameters, such as the number and arrangement of nozzles, the use of a baffle, bottom clearance, and the installation depth of the baffle; however, there was no design standard that considered the flow characteristics and light penetration of the culture media. As a result, most of the PBRs were designed on the basis of the subjective decisions of researchers and producers.

Therefore, in this study, a suitable design dimension was estimated to be able to make the best use of light efficiency in consideration of decreasing light penetration depth depending on the culture days on the assumption that the PBR with a unit module was installed in a greenhouse. Then, according to the number of nozzles, the presence or absence of a baffle installation, bottom clearance and the installation depth of the baffle, the production was predicted and analyzed using CFD. Lastly, the order of the priority of structural parameters was suggested through an analysis of the main and interaction effects between the structural parameters of the PBR to make use of it as a fundamental data.

The target PBR was designed to be feasible to produce the microalgae continuously and stably, its dimension was consisted of unit width (50 cm), depth (26 cm), and height (170 cm).

The production of microalgae with the installation of baffle which is a device of controlling fluid flow in the PBR can enhance average 41% production by

improving average light intensity and homogeneity. However, the unconditional installation of the baffle did not show the improved effect on the production cultivated in the PBR, the appropriate installation conditions (bottom clearance, installation depth, etc.) were thought to be significant. A result of analyzing the effect of the installation depth of the baffle showed that the closer the baffle was installed from the surface of light penetration, the higher the production increased. The bottom clearance showed a decreasing trend with regard to the production of the microalgae by increasing the bottom clearance.

The interaction effect between bottom clearance and installation depth among the structural parameters showed significance difference in the confidence interval 95%, other interactions among the parameters did not show the significance difference. Bonferroni post hoc test about the result of analysis of the main effect showed the significant difference in the confidence interval 99.9% with the installation depth and the bottom clearance. Additionally, the analysis result of relatively impact factor with regard to the production through the t-values showed the installation depth (-8.437^{***}), bottom clearance (-5.346^{***}), and the number of nozzles (1.975) in order.

Keyword : BPMG model, computational fluid dynamics (CFD), main effect and interaction in ANOVA, photobioreactor (PBR)

Student Number : 2013-23258

Table of contents

List of figures

List of figures

1. Introduction

Korea showed a high dependence on imported energy amounting to approximately 95% in 2014. In addition, Korea was eighth in the world regarding oil consumption and was ranked the world's fifth largest importing country (KEEI, 2014). The high dependency on oil can be a threatening factor for the national economy and energy security according to the supply and demand status of crude oil, and it has been known that there is a possibility to exacerbate abnormal weather phenomena caused by global warming depending on the combination with carbon dioxide in the combustion process of most of carbon compounds.

Thus, new and renewable energy has received attention around the globe to reduce the environmental load and secure energy independence through a gradual reduction of fossil fuel because the issue has escalated as an environmental problem for humankind; however, Korea was ranked 34th in the OCED (Organization for Economic Cooperation and Development) in terms of new and renewable energy proportions (1.7%) of primary energy because the proportion of new and renewable energy was very low (IEA, 2011). Therefore, The Korean government recently announced a plan to increases the proportion of new and renewable energy to up to 13.4% of the total amount of power until 2035, which was only 3.5% in 2013 (MOTIE, 2014).

The biomass among new and renewable energy produced in a year on earth is similar to all oil deposits, and there is no concern of this source becoming exhausted when using it properly. In particular, the bio-diesel fuel of biomass is a unique liquid fuel, and it can be utilized for large transport vehicles. Furthermore, a revised regulation regarding new and renewable energy from July, 2013, in Korea included the requirement that oil refinery companies must blend existing raw materials with bio-fuels. The existing blending ratio was 2%, and it should be increased by 2.5% until 2017 and then to 3% by 2020 (MOTIE, 2015).

Crops, timbers, and microalgae are largely used as bio-diesel resources. Microalgae, which is a third-generation biomass resource used to produce bio-diesel, contains a 1,000 times higher lipid content compared with different types of production resources in terms of the same culture area based on a rapid growth rate and has recently attracted attention.

Culture systems for microalgae are largely divided into two types: open and closed. The open system (Fig. 1(a)) is simple to enlarge for commercial production, but it is difficult to maintain the optimal culture condition due to natural environmental conditions. The closed system (photobioreactor, PBR), shown in Fig. 1(b), (c), and (d), allows for avoiding water losses and controlling culture environmental conditions artificially. It also allows for minimizing the inflow of contaminants and the loss of the carbon dioxide injected into the PBR.

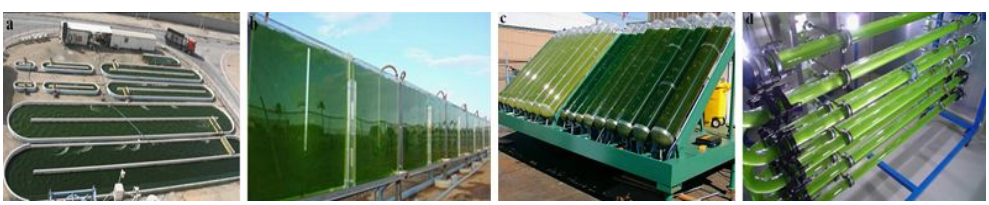

Fig. 1 Culture systems for microalgae (a) raceway pond, (b) flat-plate type, (c) inclined tubular type, (d) horizontal type. (Bitog et al., 2011)

The flat-plate photobioreactor (Fig. 1(b)) of PBRs has become known as a suitable structure for an enlargement from a number of researchers because it has a large surface area compared with its volume (S/V ratio) and has a short cycle for light and darkness. The enlargement is essential in commercialization and in securing lots of resources; however, the production of microalgae was dramatically diminished by decreasing the light penetration rate in accordance with the capacity increase (mainly, the depth of the PBR). The production of microalgae can be increased by improving the light intensity and homogeneity, which are necessary for the microalgae to photosynthesize, when designing the PBR by considering an

inner mixing characteristic. That is, the PBRs with a suitable dimension can enhance the productivity by properly considering the flow characteristics inside the PBR caused by structural parameters, such as the number and arrangement of nozzles, the use of a baffle, the bottom clearance, and the installation depth of the baffle; however, there was no design standard that considered the flow characteristics and light penetration of the culture media. As a result, most of the PBRs were designed on the basis of the subjective decisions of researchers and producers.

Methods used to measure or analyze the flow characteristics inside the PBR can be divided into field experiments using an acoustic Doppler velocimetry (ADV), a particle image velocimetry (PIV), a laser Doppler anemometer (LDA), and a numerical analysis (Peter and Anders, 2005). The ADV is a device used to observe the velocity components at a point using the effect of Doppler. But, a multi-measurement is limited due to disturbing the inner flow of the PBR because the sensor probe for observation must be placed inside the culture media while the PIV visualizes the flow field and analyzes the flow information in the interpretation area. It still has limitations in the technology used to determine the turbulent characteristics that change in a short moment and to scatter the laser by air bubble and material characteristics consisting of the PBR. In addition, the LDA, a speedometer that uses the Doppler effect, is able to measure a relatively accurate value since it does not disturb the flow field; however, the measuring equipment is extremely expensive, and the analysis of the inner flow characteristic is difficult owing to the laser scattered on surface of the PBR which consists of transparent acrylic plates or a glass materials.

On the other hand, computational fluid dynamics (CFD) can control environmental conditions and calculate numerical analysis values in the multi-point unlike field experiments in spite of requiring several steps for accuracy verification of the simulation model. Moreover, it not only excludes flow disturbance by

measuring a sensor but also allows for deliberately measuring the area of interest. In this study, a suitable design dimension was estimated to be able to make the best use of light efficiency in consideration of decreasing light penetration depth depending on the culture days on the assumption that the PBR with a unit module was installed in a greenhouse. Then, according to the number of nozzles, the presence or absence of a baffle installation, the bottom clearance, and the installation depth of the baffle, the production was predicted and analyzed using CFD. Lastly, the order of the priority of structural parameters was suggested through an analysis of the main and interaction effects between the structural parameters of the PBR to make use of it as a fundamental data.

2. Literature Review

2.1. Investigation of an optimal environment for a microalgae culture

Proper sunlight, carbon dioxide, pH, oxygen, and nutrients (N, P) are required to culture microalgae because the single-cell microorganism grows using photosynthesis and respiration. In the past, research to investigate the optimal culture conditions and to reduce the unit cost of production were carried out because among all processes (culture, harvest, extraction, and conversion), the culture process requires about 42% of the bio-diesel production cost, which is the highest compared with the other processes.

Chisti (2007) found that microalgae can accumulate and produce hydrocarbons of up to 30～70% of the dry weight under optimum growth conditions. The variables of the culture conditions influencing bio-diesel production include culture temperature, cell concentration, pH, CO_2 concentration, aeration rate, and light.

Fabregas et al. (1998), Oh and Rhee (1991), Degen et al. (2001), Kalacheva et al. (2002), Sostaric et al. (2009), Choi et al. (2011), Chinnasamy et al. (2009), and Park et al. (2010) investigated the optimal culture conditions (temperature, artificial seawater concentration, initial pH, CO_2, etc.) for a variety of microalgae species to improve the specific growth rate of the microalgae. Park et al. (2010) investigated the optimal culture conditions regarding the culture temperature, artificial seawater concentration, pH, CO_2 concentration for *Nannochloropsis oculata* and confirmed the optimal culture conditions at 3% artificial seawater, an initial pH of 8.5, and a temperature of 25℃. In addition, although the dry cell weight was 0.76 g/L when CO_2 was not supplied, after injecting 5% CO_2, the dry weight increased to almost double by 1.5 g/L (Fig. 2). Choi and Lee (2011) experimented with a change in the rate of increase for *chlorella vulgaris* according to the temperature, light intensity,

and pH. The results showed that the optimal culture temperature was 25～30 ℃, which is similar to Park et al. (2010), and the optimal pH was 7～7.5. Also, they mentioned that the growth rate for *chlorella vulgaris* during the culture period slowly increased for 5 days, and from 5 to 16 days, it showed an explosive increase. After day 16, there was not much growth.

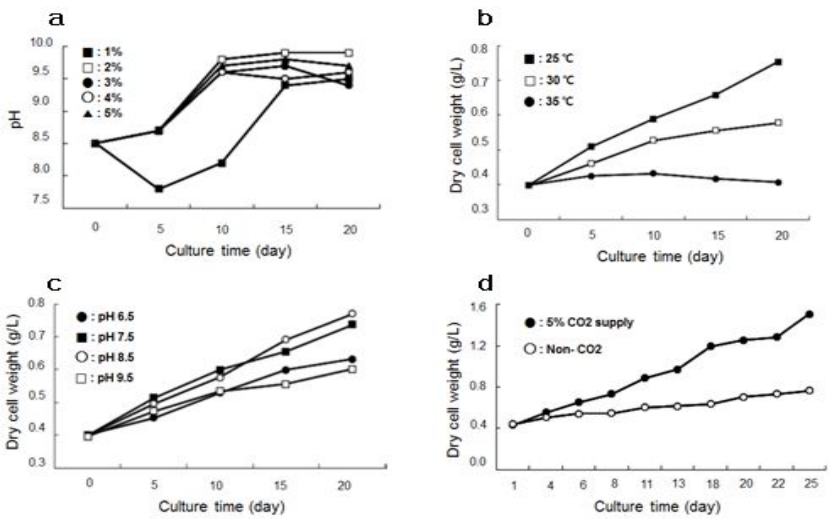

Fig. 2 Effects of artificial seawater contents on the growth of *Nannochloropsis oculata* (a), influence of temperature on the growth (b), influence of initial pH on the growth (c), effect of CO_2 on the growth (d) (park et al., 2010)

However, light condition was known as the most important condition to control microalgal growth among the many environmental conditions (Merchuck et al., 2003). The microalgae in dense concentrations utilized more light for photosynthesis, but excessive light intensity caused photo-inhibition, which impeded its growth.

Kitaya et al. (2005) investigated the optimal light intensity among six levels of light intensity (20~200 μmol $m^{-2}s^{-1}$) culture conditions of *Euglena gracilis* under conditions with 5 different temperatures (25~33℃) and three different CO_2 concentrations (2~6%). The cells were highest at the light intensity of 100 μmol m^{-}

$^{2}s^{-1}$ under the temperature of 27~31℃ and CO_2 concentration of 4%, which is similar to other research. The other researches related to the conditions of the light intensity were listed in Table 1.

Table 1 Suitable culture condition according to microalgal species

Species	Light intensity (μmol $m^{-2}s^{-1}$)	Temperature (℃)	pH	CO_2 (%)	Ref.
Euglena gracilis	100	27~31	-	4	Kitaya et al., 2005
Chrollera vulgaris	100~150	25-35	7~7.5	-	Choi and Lee, 2011
Spirulina platensis	200	-	9-10	-	Oncel and Akpolat, 2006
P.purpureum	120	25	7	-	Baquerisse et al., 1999
Chrollera vulgaris	120	-	-	-	Li et al., 2012
Dunaliella	300	32	6	1-2	Auken and Nulty, 1973
S.Dimorphus	120	29	8.5	4	Kong et al., 2007
Nanochloropsis sp.	100	-	-	-	Wahidin et al., 2013
Selenastrum minutum	420	35			Bouterfas et al., 2002
Coelastrum microporum	400	35			Bouterfas et al., 2002
pyrennoidosa	250	37		5	Ogbonna et al., 1996

Qiang and Richmond (1996) quantitatively evaluated the effect of the mixing rate, the cell concentration of microalgae, and the light intensity for *spirulina platensis* on microalgae productivity and showed that the productivity and efficiency of the photosynthesis can be maximized in the condition of an optimal mixing rate and the concentration of microalgae. On the other hand, they were required to carefully consider the mixing rate because a mixing rate that was too

high destroyed the cells and a mixing rate that was too low reduced the efficiency of the productivity.

2.2. Structural parameters influencing the flow characteristic inside the PBR

Research that investigated an optimal culture on a small scale, such as using a flask and beaker, was conducted initially. Afterward, mixing characteristics became important in increasing the scale of the culture because the growth of microalgae is significantly influenced by the distribution of light for photosynthesis within the PBR (Luo et al., 2003; Huang et al., 2015). Microalgae are known to be able to improve productivity when maintaining the suitable frequency of light exposure because they are a single-cell organisms that grow based on photosynthesis. Therefore, it is necessary to harmonize the biological and rheological properties appropriately in the PBR design (Pruvost et al., 2006). To increase the frequency of the light exposure, research related to a mixing improvement inside the PBR has been conducted. Suzukiu et al. (1995) considered the hydrodynamic shear force as one of the important factors in the growth of microalgae. Structural parameters affecting the hydrodynamic characteristics inside the PBR can be the number of nozzles, the location of baffle installation, and so on.

One of the most commonly used methods to improve the inner flow characteristics is to install a baffle. Zhang et al. (2013) showed that a PBR with a baffle improved the production by 29.94%, they thought the baffle intensified the mixing performance and improved the mass transfer efficiency in the culture media. Huang et al. (2015) conducted a numerical simulation and field experiment in terms of compositions for the baffle and the existence of the baffle within the flat-plate PBR. The results of the culture experiment showed that a split flat-plate airlift reactor has 0.018 g/L in the specific growth rate. They described it as 50%, which is 12.5% higher compared with a bubble column and a central flat-plate airlift PBR, respectively (Fig. 3 and Table 2). Based on these results, to install a baffle implied

that it can affect the productivity of microalgae by improving the mixing performance and the mass transfer rate between the liquid and gas; however, the increase of the installation depth of the baffle was known to be able to cause a reduction in the driving force inside the PBR because a portion of the injected gas from the nozzles directly influences the downcomer (Fig. 4). Also, Huang et al. (2015) described that the installation depth can influence inner flow of the culture media as well as it can affect the local swirl flow in the PBR; thus, they emphasized to optimize the installation depth.

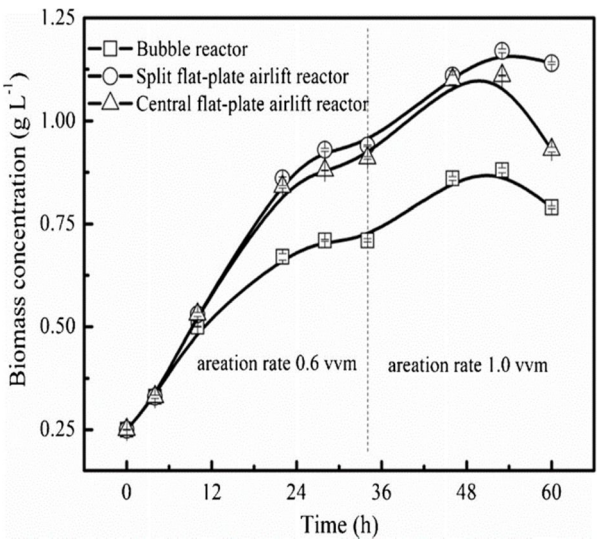

Fig. 3 Comparison of *C. pyrenoidosa* growth in the three types of PBRs (Huang et al, 2015)

Table 2 Results of the photoautotrophic cultivation of *C. pyrenoidosa* in the three types of flat-plate PBRs

Reactor type	Maximum biomass concentration ($g \cdot L^{-1}$)	Specific growth rate (h^{-1})	Biomass productivity ($g \cdot L^{-1} \cdot h^{-1}$)
Bubble reactor	0.882±0.006	0.024±0.00013	0.012±0.00011

Split flat-plate airlift reactor	1.168±0.005	0.029±0.00002	0.018±0.00003
Central flat-plate airlift reactor	1.110±0.011	0.028±0.00008	0.016±0.00009

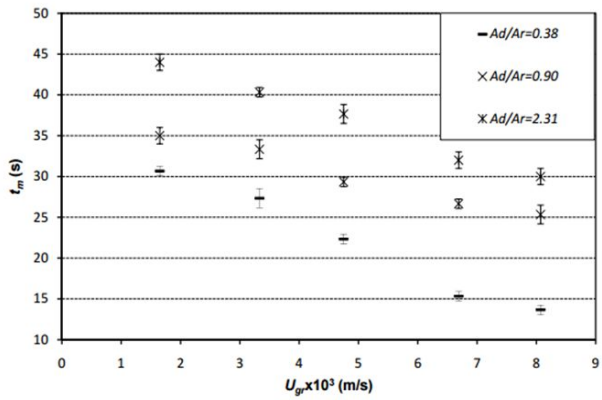

Fig. 4 The effects of riser and downcomer on mixing time (Huang et al., 2015)

The effect of top clearance, which is a distance from the top edge of the baffle to the level of the medium, and bottom clearance, which is the distance from the bottom surface of the PBR to the lower edge of the baffle, can vary considerably on the assumption that the injection rate is equal. Luo and Al-Dahhan (2008) demonstrated that the size of the top and bottom clearance significantly affect energy dissipation in the top and bottom regions and influence the overall flow characteristic and mixing environment. Huang et al. (2015) measured the distribution of the flow rate and found that the higher the top clearance, the bigger the flow velocity in the downcomer (Fig. 5). They also analyzed the various bottom clearances by measuring the mixing time, and the mixing time decreased by increasing the bottom clearance. It is speculated that a result of recycling the fluid from the downcomer to riser was important (Huang et al., 2015). Yakubu and Gumery (2010) also indicated that increasing the bottom clearance increased the

liquid velocity because the pressure drop at the bottom was strongly affected. In particular, Yu et al. (2009) mentioned that the optimal bottom clearance was in the rage of 2 ~ 6 cm. Furthermore, Chisti (1989) announced that the influence of the bottom clearances on mixing between ranges mentioned above was not pronounced.

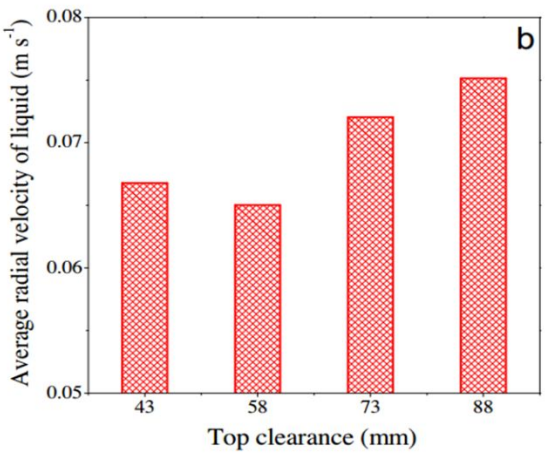

Fig. 5 Average radial velocity of liquid ($m \cdot s^{-1}$) according to top clearance (Huang et al., 2015)

An et al. (2011) showed that a suitable design for the air injection nozzle in the PBR can increase the production of the microalgae and the survival rate by increasing the number and diameter of nozzles because of the reduction in the bubbling period and the bubble flow rate. They also suggested that the number of nozzles and the diameter of nozzles can be calculated to generate uniform bubbles inside the PBR to prevent damage to the cells by the bubbles and fluid shear force. The nozzle is a parameter used to adjust the speed of air and nutrients injected into the PBR. It is important to estimate the number of nozzles for a suitable number depending on the capacity of the PBR because the largest cell destruction area has known around the nozzle holes injected with the bubbles and nutrients.

Barbosa et al. (2003) showed that the change of the cell concentration of the

microalgae generated by the number of injection nozzles (1 or 9) installed in the PBR is a relative concentration concept and measured the death rate of the microalgae according to the number of nozzles in the same PBR. From the results, they highlighted the necessity of the suitable installation of the nozzles in the design of the PBR by quantitatively analyzing the death rate (0.047±0.16 h^{-1} per hour) when there was one injection nozzle, while the death rate was almost 0 when there were nine injection nozzles (Fig. 6).

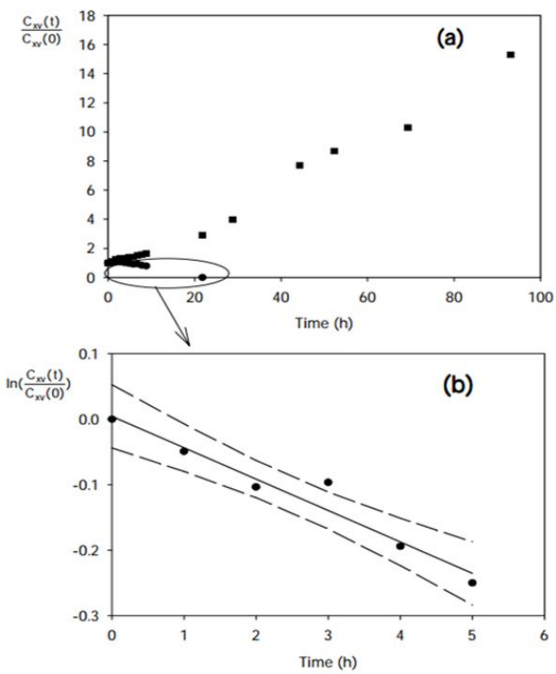

Fig. 6 Growth curve depicted as the variation in the number of viable cells of *D. tertiolecta* cultivated batchwise in a lab-scale bubble column with a different number of nozzles in the sparger: (●) one nozzle and (■) nine nozzles. Superficial gas velocity 0.034 ms^{-1}. (b) parameter K_d estimated for the experiment with one nozzle as 0.047±0.016h^{-1}:(●) experimental data; (-) relationship estimated by linear regression; and (--) 95% confidence interval (Barbosa et al., 2003)

Nozzle size was also used as a parameter to improve the mixing characteristics inside the PBR. Merchuk et al. (1998) conducted extensive research

with seven different nozzles of varying sizes. They mentioned that the size of the nozzle diameter had an impact on the gas holdup and liquid recirculation. Bitog et al. (2012) deduced a suitable nozzle size by analyzing the ratio of the formation of the dead zone that occurred in the PBR according to the nozzle size installed in the PBR, and they showed that the diameter size of the nozzle plays an important role in the circulation time inside the PBR. Jhawar and Prakash (2014) investigated the mixing effect and mass transfer between the gas and liquid phases according to the difference of the diameter of the nozzles installed in the bubble column. Also, Zhang et al. (2015) analyzed the effect of changing the number of nozzles and the diameter of nozzles and stated that nozzles can affect the flow in the culture media and growth rate.

2.3. Methods for evaluating the performance of PBRs

Axial and radial mixing of the liquid phase in the PBR can be characterized by dispersion coefficients; however, Deckwer (1992) described that the radial dispersion coefficient is always less than one-tenth of the value of the axial coefficient; thus, the radial dispersion coefficients can be negligible. Therefore, the axial dispersion coefficient is used as a method to evaluate the mixing performance in the axial direction of the PBR. This is a function of permeability inside the PBR caused by bubbling, the structure of the reactor, and the fluid characteristics (Ohki and Inoue, 1970; Rubio et al., 2004). The equation is as follows:

$$C_T = 1 + 2\sum_{m=1}^{m=\infty} \cos(m\pi y)\, e^{(-m^2\pi^2\theta)} \qquad \text{Eq. (1)}$$

Where,

C_T : Value of tracking materials concentration (Dimensionless constant)

y : Coordination in terms of axial direction

θ : Time (Dimensionless constant)

This method is classified as an indirect method used for evaluating the performance of the PBR by calculating the change of the concentration of the tracer materials on the direction of the axial according to the time.

Mixing time can be considered one of the most important factors in designing the PBR. Homogeneous mixing formed in the PBR decreased the death rate and mutual shading between cells of microalgae, and simultaneously increased the frequency exposed to sunlight. As a result of this, it reduced the possibility of photo-inhibition and stimulated a mass transfer rate between microalgae particles and carbon dioxide (Janvanmardian and Palsson, 1991). Mixing time is the time demanded until the concentration of any substance sprayed into culture media become constant and has been generally defined as the time required to attain a 5%

deviation from complete homogeneity after injecting a tracer substance into the PBR (Ugwu et al., 2008; Rubio et al., 2004). To estimate mixing time, tracer substances are commonly used. In addition, the signal-response method using a pH electrode is also used (Rubio et al., 2004; Ugwu et al., 2003; Pruvost et al., 2006). The acid tracer method is used for measuring the mixing time and is calculated as a dimensionless concentration after injecting mainly a hydrogen ion, as shown in Eq. (2).

$$C_T = \frac{[H^+]_x - [H^+]_{ini}}{[H^+]_f - [H^+]_{ini}} \quad \text{Eq. (2)}$$

Where,

C_T : Value of tracing materials concentration

H^- : Tracer concentration of hydrogen (Dimensionless constant)

Pruvost et al. (2006) and Sato et al. (2006) evaluated mixing time in a torus photobioreactor using CFD and considered the difficulty of maintaining uniform conditions in the field experiment and the limitation of measuring from multiple points. Seo et al. (2012) divided inner volume of a cylinder-type PBR into 3 parts with the starting point as the center (0～35 mm, 35～65 mm, 65～85 mm), generated tracer materials from each part using CFD, and then calculated the mixing time when the concentration of the trace materials was constant (Fig. 7).

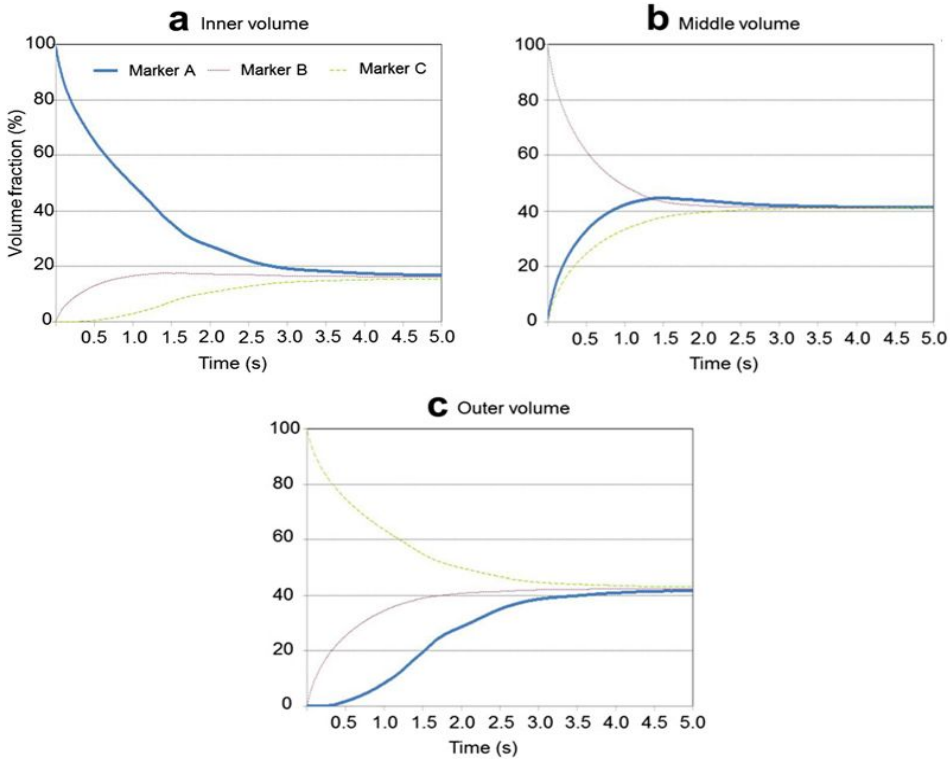

Fig. 7 CFD-computed volume fraction of three markers according to their location for each volume (Seo et al., 2012)

A dead zone is caused by the hydrodynamic characteristics inside the PBR. Yu et al. (2009) defined the dead zone as a stagnant region when the flow velocity is below 0.001 $m \cdot s^{-1}$ in the PBR. There is little growth of microalgae in this area because most of the microalgal cells were deposited in the bottom of the PBR, and the metabolism also dramatically decreased. Bitog et al. (2014) established the optimal environmental conditions compared with the formation of the dead zone among 32 cases that consisted of air flow rates (0.05, 0.10, 0.15 and 0.20 v/v/m), nozzle diameter size (5, 10, 15, 20 mm), and the presence or absence of the baffle. They also found that the formation of the dead zone in the PBR decreased when the air flow rate was higher and the nozzle diameter was smaller (Table 3)

).

Table 3 Volume percentages of dead zones of the 32 CFD simulations (Bitog et al., 2014)

Case	Volume percentage of dead zones, %	Average circulation time, S	Case	Volume percentage of dead zones, %	Average circulation time, S
$A_1B_1C_1$	8.21	14.88	$A_3B_1C_1$	6.61	14.05
$A_1B_1C_2$	3.66	9.21	$A_3B_1C_2$	3.12	8.41
$A_1B_2C_1$	18.86	19.57	$A_3B_2C_1$	6.31	15.55
$A_1B_2C_2$	11.41	13.81	$A_3B_2C_2$	4.18	9.51
$A_1B_3C_1$	34.58	25.66	$A_3B_3C_1$	14.88	18.51
$A_1B_3C_2$	26.61	20.01	$A_3B_3C_2$	9.51	13.67
$A_1B_4C_1$	42.51	26.89	$A_3B_4C_1$	26.66	21.41
$A_1B_4C_2$	33.67	22.81	$A_3B_4C_2$	18.85	15.66
$A_2B_1C_1$	7.08	15.65	$A_4B_1C_1$	5.24	13.84
$A_2B_1C_2$	3.12	9.05	$A_4B_1C_2$	2.87	8.05
$A_2B_2C_1$	11.01	16.21	$A_4B_2C_1$	9.51	15.01
$A_2B_2C_2$	4.87	10.08	$A_4B_2C_2$	4.65	9.29
$A_2B_3C_1$	22.21	20.51	$A_4B_3C_1$	13.67	17.22
$A_2B_3C_2$	14.61	14.48	$A_4B_3C_2$	8.11	12.41
$A_2B_4C_1$	29.81	22.31	$A_4B_4C_1$	20.08	19.88
$A_2B_4C_2$	20.67	17.71	$A_4B_4C_2$	11.66	13.91

A: Air flow rates of 0.05, 0.10, 0.15 and 0.20 v/v/m corresponding to A_1, A_2, A_3 and A_4, respectively

B: Nozzle size diameter of 5, 10m 15 and 20 mm corresponding to B_1, B_2, B_3 and B_4, respectively

C: PBR geometry without baffle and with baffle corresponding to C_1 and C_2, respectively

The BPMG model has newly been developed to predict statistical biomass production by Seo et al. (2014). The main principle is the convergence between the growth model of the microalgae based on the light intensity the microalgae absorbed and time-dependent particle tracking occurred by inner fluid flow inside the PBR. That is, the BPMG model, a model used to evaluate the performance of the PBR regardless of the shape or size of the PBR, is available to directly predict the production of the microalgae by considering a flow characteristic that was occurred by injecting air bubbles inner structures in the PBR as well as the growth model for the microalgae simultaneously.

3. Materials and Methods

Although the productivity of a microalgal culture can be enhanced by taking into account the mixing characteristics, most photobioreactors have been made based on subjective decisions of researchers or producers in the absence of a criteria for a standard design or guidelines of them. Therefore, first, the design dimension was chosen to make the best use of light efficiency in consideration of decreasing the light penetration depth depending on the number of culture days based on the assumption that the PBR with a unit module was installed in a greenhouse.

Second, a review of the literature focusing on the structural characteristics that affect the mixing characteristics was analyzed, and the structural characteristics that affect the mixing characteristics were set with parameters based on preceding studies. Then, the CFD simulation model was designed because mixing characteristic within the PBR is important for microalgae production by improving the frequency of light exposure that the microalgae absorb in the growth process and the response speed of metabolism. Here, material properties, such as surface tension and boundary conditions (grid size, time step interval, multi-phase model, etc.), which were verified by Seo et al. (2012), were applied in the simulation models.

Third, the microalgae production was calculated in accordance with the condition of the structural parameters, such as the number of nozzles, nozzle arrangement, baffle installation, bottom clearance of the baffle, and installation depth of the baffle. Then, the effect of the installation of the baffle was investigated on the basis of the predicted production.

Next, a statistical analysis was conducted on the structural parameters and the predicted production according to the structural parameters using SPSS (IBM SPSS Statistics 23.0). Even though several researchers conducted statistical analyses in

existing research, most researchers deduced the regression formula between the environmental parameters and microalgal production in a limited model or analyzed a simple correlation analysis. In this study, the applied method for the statistical analysis was a two-way ANOVA. With this method, the main effect of the relative influence among the structural parameters was evaluated by analyzing the influence of the dependent variable depending on the change of an independent variable. The interaction effect was analyzed for multiple effects, and more than two independent variables were investigated. In addition, a Bonferroni post hoc test, which is an effective method for comparing a small population, was implemented in case of a statistically significant difference. Fig. 8 contains a brief flowchart summarizing the research process of this study.

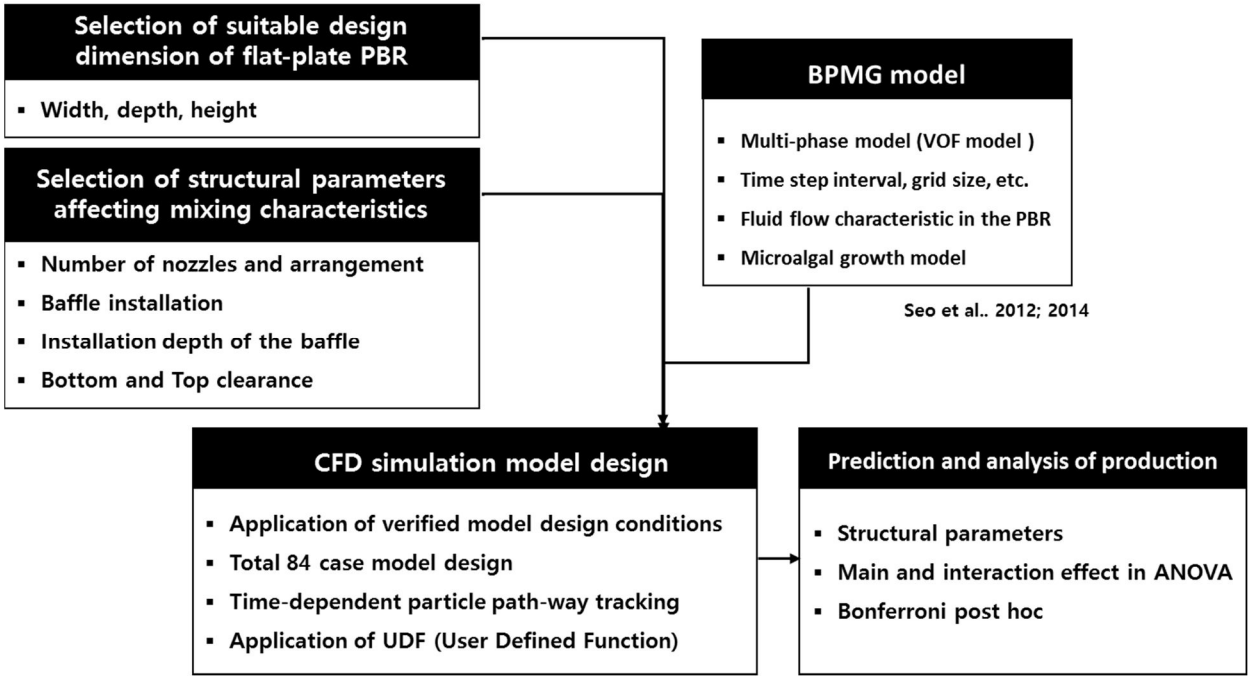

Fig. 8 Research flow for predicting production and the statistical analysis

3.1. Microalgae

Microalgae, single-cell organisms living in water that grow based on photosynthesis, are known to include at least 50,000 species on earth. Microalgae use sunlight, nutrients (N, P), and carbon dioxide (1.8 ton carbon dioxide use per microalgae 1 ton), etc., as energy sources for growth. They can be utilized in a purification process of wastewater, such as industrial and agricultural wastewater, as well as in the reduction of carbon dioxide emission because they consume nutrients (N, P) which are a cause of water pollution and carbon dioxide in the process of production. In general, microalgae have a higher productivity than any other bio-diesel resources on the basis of a rapid growth rate. They can be cultured in harsh environment conditions, such as high salinity and strong alkali; however, microalgae growth characteristics and cell components are significantly different depending on the culture form. A typical growth curve of microalgae is shown in Fig. 9.

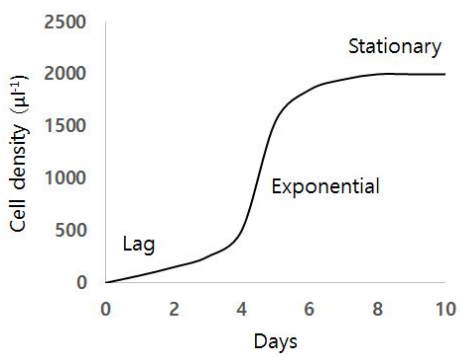

Fig. 9 Phase in the typical growth of microalgae culture (FAO, 2014)

The growth phases were classified as lag, exponential, stationary, and death phase. The lag phase is a period for the microalgae to adapt in a new culture environment. There is little growth in this period. Then, the growth phase leads to the exponential phase in which the cellular multiplication of the microalgae was

increased, as this is the most active period of growth that is similar to an exponential function. After that, the cells confront biochemistry changes from limitation factors to growth. They proceed to the death phase when the growth is almost 0 and when microalgae in the stationary phase cannot sustain metabolism.

3.2. Design of culture systems

Systems for microalgae culture are largely divided into two types. One is an open culture system using the natural environment, the other is a closed culture system controlling the growth environment artificially. The open culture system involves installing a production facility in a natural environment, such as an open pond or raceway pond (Fig. 1(a)). It is easy to maintain and enlarge for commercial production, but it is difficult to control the CO_2 concentration, light conditions, pH, temperature, etc., for optimal production of the microalgae because only an outdoor natural environment is used. In addition, there is the drawback of high losses of water due to evaporation in the atmosphere, and there is less productivity per unit area compared with the closed culture system. Furthermore, Yoo et al. (2009) insisted that South Korea only has 3 or 4 months to utilize the open culture system in consideration of 4 clearly compartmental seasons, and it is not suitable to install a culture system considering the geographical conditions consisting of almost 60% mountainous areas. Also, there were limitations for enlargement and commercialization because the depth of a pond can be limited in consideration of light penetration depth as well as the inflow possibility of the contaminants to the culture medium.

On the other hand, the closed systems can avoid water losses and control the culture environmental conditions artificially. It also allows for minimizing the effect of contaminants and the loss of the carbon dioxide injected into the closed culture system. The closed culture system varies depending on the shape and operation method, such as a tubular PBR, plate PBR, horizontal PBR, spiral type PBR, etc. The flat-plate PBR which was developed by Milner in 1953 is the most common type. It is known for having a suitable structure for enlargement due to the wide surface area for unit volume (Xu et al., 2009; Sierra et al., 2008; Su et al., 2010). The names of each part of the PBR are shown in Fig. 10.

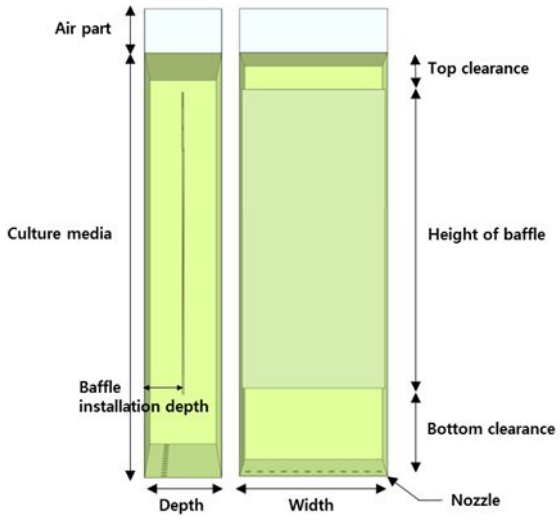

Fig. 10 Name of each part and schematic diagram of Flat-plat PBR

Mixing gas (CO_2 and O_2) was injected into the culture media of a flat-plate PBR through the nozzles (Fig. 11). The flow inside the PBR was irregularly formed by the injected CO_2 and O_2 from the nozzles because the frequency of the light of the microalgae growth based on the photosynthesis was significantly altered, and the inhomogeneity of light intensity for the microalgae to absorb was also aggravated. To resolve the problems, the baffle (fluid control device) was installed in the flat-plate PBR. The installation of the baffle not only influenced the mass transfer rate and mixing for the CO_2 and O_2 in the PBR, it also enhanced the growth of the microalgae by improving the frequency of the light (Degen, 2001; Ugwu et al., 2002; Wang and You, 2013; Seo et al., 2014).

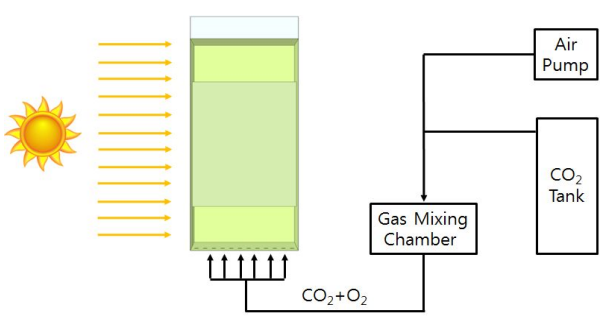

Fig. 11 Schematic diagram of operating system of photobioreactor

3.3. Computational Fluid Dynamics (CFD)

Computational Fluid Dynamics (CFD) uses the Navier-stokes equation, which is a governing equation dealing with the fluid flow problem. It is a technique used to solve mass and momentum using an energy conservation equation on the each grid and interpreting them (Yeo et al., 2015). The CFD was largely divided into 3 parts: 1) a pre-processing step to design the appearance of the model and to make the mesh of analysis domain, 2) a main operation step to solve the equation by the method of numerical analysis on the interpretation area of the designed model after the discretization process, and 3) a post processing step to analyze the results of the simulation visually. In this study, DesignModeler (ver. 15.0., ANSYS Inc., USA), which is a commercial program used as a tool for the preprocessing step, was used to form the basic appearance and a finite number of grids, and the model was designed by designating the boundary conditions. Once the target area was designed as a model with a three-dimensional volume, mass, momentum, the energy conservation equation related to the movement of fluid and energy was applied in the each grid and calculated after the discretization processes. The mass, energy, and momentum conservation equation are shown in Eqs. (3) ~ (5).

Mass conservation equation:

$$\frac{\partial \rho}{\partial t} + \nabla \cdot (\rho \vec{v}) = S_m \qquad \text{Eq. (3)}$$

Energy conservation equation:

$$\frac{\partial}{\partial t}(\rho E) + \nabla\big(\vec{v}(\rho E + P)\big) = \nabla\big(k_{eff}\nabla \mathrm{T} - \sum h\vec{J}_i + \big(\vec{\tau}_{eff}\vec{v}\big)\big) + S_h \qquad \text{Eq. (4)}$$

Momentum conservation equation:

$$\frac{\partial}{\partial t}(\rho\vec{v}) + \nabla \cdot (\rho\vec{v}\vec{v}) = -\nabla P + \nabla(\bar{\tau}) + \rho\vec{g} + \vec{F} \qquad \text{Eq. (5)}$$

Where,

E : Total energy ($kg \cdot m^2 \cdot s^{-2} \cdot kg^{-1}$)

ρ : Density ($kg \cdot m^{-3}$)

$\vec{v}$: Velocity ($m \cdot s^{-1}$)

P : Static pressure ($kg \cdot m^{-1} \cdot s^{-2}$)

$\bar{\tau}$: Stress tensor ($kg \cdot m^{-1} \cdot s^{-2}$)

$\bar{\tau}_{eff}$: Effective stress tensor ($kg \cdot m^{-1} \cdot s^{-2}$)

$\vec{g}$: Gravitational acceleration ($m \cdot s^{-2}$)

$\vec{F}$: External force vector ($kg \cdot m \cdot s^{-2}$)

S_m : Mass source term by chemical reaction ($kg \cdot m^{-2}$)

k_{eff} : Effective conductivity ($kg \cdot m^{-1} \cdot s^{-3} \cdot K^{-1}$)

$\vec{J}_i$: Component of diffusion flux

S_h : Enthalpy rise by chemical reaction or radiation ($kg \cdot m^{-1} \cdot s^{-3}$)

Recently, performances and techniques of computers have been improved, so the computing time in the interpretation area was significantly reduced and the accuracy was also enhanced because it was feasible to apply and compare a variety of turbulence models with the environmental conditions.

3.4. Biomass Production prediction grafting Mixing and Growth model (BPMG model)

The BPMG model was developed by Seo et al. (2014) to evaluate the performance of photobioreactors. It considers the hydrodynamic characteristics in a PBR and the microalgal growth model, which consists of the light intensity that the microalgae absorb inside the PBR. With this method, the production of a target PBR can be directly predicted regardless of the shapes and capacities of the PBRs by tracking the particle pathway of the microalgae considered with the hydrodynamic characteristics that occur due to the air injection into the PBR and the growth model for the microalgae at the same time. The calculation procedure for the BPMG model is shown in Fig. 12.

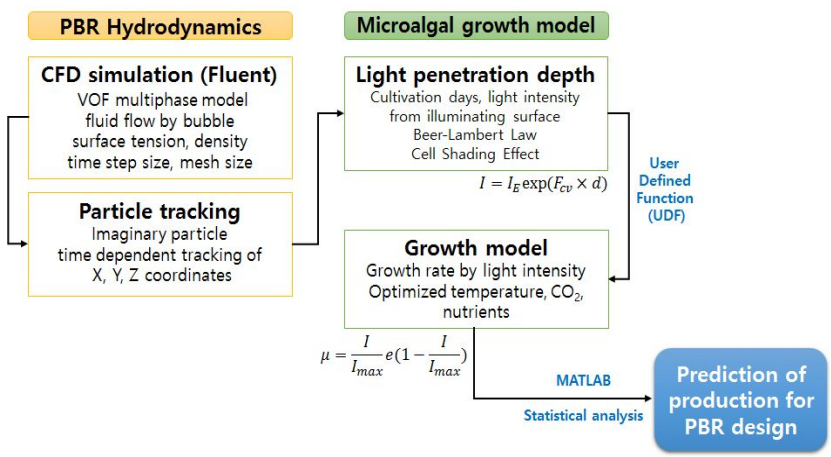

Fig. 12 Calculation procedure of the BPMG model (Seo et al., 2014)

The BPMG model interprets the fluid flow that occurs due to bubbles and inner structures in the PBR using volume of fluid (VOF) tracked particles that behave in accordance with hydrodynamic characteristics (Seo et al., 2014). The VOF model is a method used to track the boundary surface between multi-phases in a fixed Eulerian grid system. When two types of immiscible fluids form the boundary surface, it is applied. The boundary surface of the phase presents a

function defined as 0 or 1 of the volume fraction of each cell (ANSYS INC, 2014).

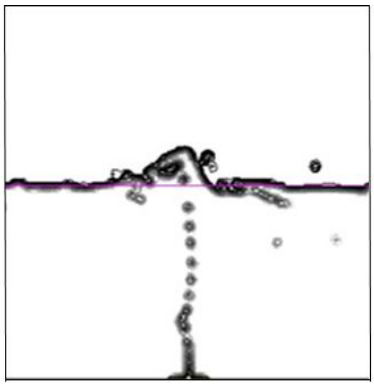

Fig. 13 illustration of the VOF model realization (Seo et al., 2012)

The VOF model uses a momentum equation (Eq. 6) and a volume fraction (Eq. 7) as governing equations. It is possible to predict the flow of large air bubbles in the liquid because the infiltration does not happen between phases because the model calculates the flow by tracking the surface of each phase. Also, the fluid flow that occurs due to each bubble can be presented as a momentum equation (Eq. (6)), and the change of the boundary surface among the multi-phases can be tracked by solving the continuity equation for the volume fraction of the phase (Eq. 7).

$$\frac{\partial}{\partial t}(\rho\vec{v}) + \nabla\cdot(\rho\vec{v}\vec{v}) = -\nabla \mathrm{p} + \nabla\cdot\left[\mu\left(\nabla\vec{v} + \nabla\overrightarrow{v^{T}}\right)\right] + \rho\vec{g} + \vec{F} \qquad \text{Eq. (6)}$$

$$\frac{1}{\rho_q}\left[\frac{\partial}{\partial t}\left(\alpha_q\rho_q\right) + \nabla\cdot\left(\alpha_q\rho_q\overrightarrow{v_q}\right) = S_{\alpha_q} + \sum_{p=1}^{n}(\dot{m_{pq}} - \dot{m_{qp}})\right. \qquad \text{Eq. (7)}$$

Where,

$\vec{v}$: Velocity of mixture ($m\cdot s^{-1}$)

μ : Coefficient of viscosity ($kg\cdot m^{-1}\cdot s^{-1}$)

$\vec{g}$: Gravitational acceleration ($m\cdot s^{-2}$)

$\vec{F}$: Volumetric forces at the interface resulting from the tension

m_{qp} : Mass transfer from phase q to phase p

$\dot{m_{pq}}$: Mass transfer from phase p to phase q

S_{α_q} : Source term

α_q : Volume fraction of phase q

ρ_q : Density of phase q (kg·m^{-3})

$\overrightarrow{v_q}$: Velocity of phase q

However, it is difficult to design a model, and it may require considerable time because a more intensive grid design is needed since only one phase can exist in each grid (Seo et al., 2014). After computing the light intensity in accordance with the location of particles on the basis of a moving path of the tracked particle at regular intervals. The specific growth rate can be computed by assigning the light intensity to Eq. 8.

$$\mu = \frac{I}{I_{opt}} \exp(1 - \frac{I}{I_{opt}}) \quad \text{Eq. (8)}$$

Where,

μ : Growth rate by light intensity

I : Light intensity (μmol m^{-2}s^{-1})

I_{opt} : Optimum light intensity for microalgae culture (μmol m^{-2}s^{-1})

3.5. Analysis of variance (ANOVA)

The analysis of variance (ANOVA), a statistical method used to test differences with two or more means, is lexically defined as an analysis method used to generalize a t-test. It is a method of analyzing the factors that have a significant effect compared with errors by dividing the sum of the square into the sum of the square per each factor. As a technique analyzing the relation between an independent variable and a dependent variable, there are a one-way ANOVA based on an independent variable, a two-way ANOVA based on two or more than two independent variables, and a multi analysis of variance (MANOVA) used to verify the differences between two or more groups in related situations by expanding the analysis of variance.

If significance probability (p) is below α, the results show a statistical significance in the significance level. This means that the intensity of contrary evidence for a null hypothesis is larger than the designated level. That is, if the significance probability from the results is lower than the significance level α, it can describe the analysis results that showed a statistically significant difference.

For example, a significance probability lower than 0.05 ($p<.05$) means that 95% of the analysis is reliable and the other 5% is not. Also, a significance probability lower than 0.01 ($p<.01$) means that 99% of analysis is reliable and the other 1% is not. The significance probability $p<.001$ can be interpreted in a like manner. The smaller the range of the significance level, the more intensive the analysis can be. In general, when the significance probability is below the designated significance level .05, the analysis results can describe a statistically significant difference.

3.6. Experimental procedures

3.6.1. Structural design of the flat-plate PBR for CFD modelling

Microalgae require a suitable light condition, carbon dioxide, pH, oxygen, and nutrients (N, P) for the microalgal culture process. In particular, the light condition plays an important role since microalgae grow on the basis of photosynthesis.

Light transmissivity inside the PBR according to the culture days is the same as is shown in Fig. 14. A PBR with a proper depth is sufficient to supply a suitable light intensity for miroalgal growth due to low cell density during the initial culture period. As time goes by, the part of the PBR showing a maximum specific growth rate was restricted. That is, in a part of the PBR, the sufficient light supplied dramatically decreased, and no growth area was observed. Therefore, the proper depth to sustain the maximum growth rate in the high cell densities must be estimated.

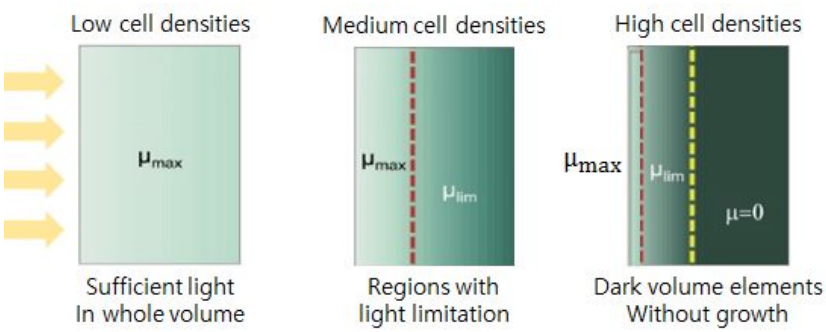

Fig. 14 Schema of light conditions in a plate photobioreactor illuminated from one side at different cell densities, with maximum growth rate, light limited growth rate, no cell growth (Anna et al., 2012)

The relationship between the light intensity and the specific growth rate with distance from wall that the light penetrated was shown in Fig. 15. (Merchuk and Wu, 2003). I_2 was defined as the point that the light was supplied to retain the

survival of the microalgae, and the light intensity until I_1 constantly maintained the maximum microalgal growth. Also, a light intensity less than I_1 was observed to sharply decrease the growth rate of the microalgae.

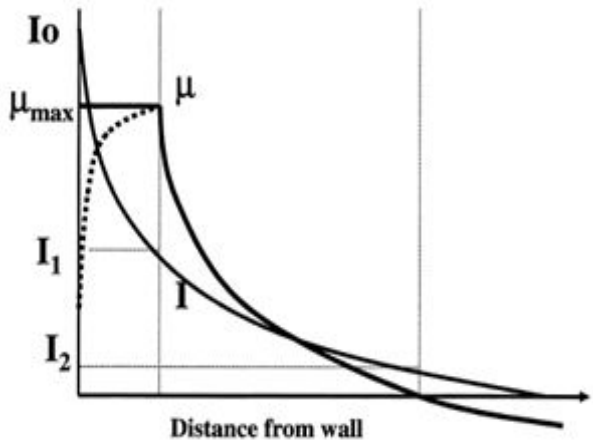

Fig. 15 Correlation among light intensity, specific growth rate, and distance from the wall for the photobioreactor (Merchuk and Wu, 2003)

Where,

I_o : Initial light intensity on the surface of photobioreactor

I_1 : Minimum light intensity to maintain maximum growth rate

I_2 : Minimum light intensity to maintain microalgal growth

μ : Growth rate

μ_{max} : Maximum growth rate

A growth model among various growth models (Table 4) similar to a culture experiment, which was conducted from Seo et al. (2012), was selected. Then, a light intensity of 100~350 $\mu Em^{-2}s^{-1}$ was applied in the selected growth model, and the minimum light intensity needed to maintain the maximum growth rate was estimated. A distribution of light intensity for the depth inside the PBR was analyzed by the Lambert-Beer's law on the estimated light intensity, and the depth sustaining 250 $\mu Em^{-2}s^{-1}$ light intensity was estimated when the concentration of the

microalgae was the highest prior to harvest. Here, the extinction coefficient accounting for water was 2.5 ml m^{-1}/106 cell, and the self-shade effects between cells (k_w) were applied for 0.2 m^{-1} (Seo et al., 2014).

Table 4 Models for light-dependent specific growth rate

Equation	Reference
$\mu = \frac{\alpha \mu_{max} I}{\mu_{max} + \alpha I}$ Eq. (9)	Tamiya et al. (1953)
$\mu = \mu_{max}(1 - e^{-\frac{I}{I_{max}}})$ Eq. (10)	Van Oorshot (1955)
$\mu = \frac{I}{I_{max}} e^{(1-\frac{I}{I_{opt}})}$ Eq. (11)	Steele (1977)
$\mu = \frac{\mu_{max} I^n}{I_k^n + I^n}$ Eq. (12)	Molina Grima et al. (1994)

$$I = I_E \exp[-(k_x \times x + k_w)d \quad \text{Eq. (13)}$$

Where,

I : Instantaneous incident light intensity on the cells (μE m^{-2} s^{-1})

I_E : External irradiance on the PBR surface (μE m^{-2} s^{-1})

k_x : Extinction coefficients accounting for water (m^{-1})

k_w : Self-shade effects between cells (m^{-1})

x : Biomass concentration (106 cells mL^{-1})

d : Radial distance from the cell to the illuminated surface (m)

For the height of the flat-plate PBR, refer to the standard design document of a glass-covered greenhouse based on the assumption of installing the flat-plate PBR inside the glass-covered greenhouse.

3.6.2. Design of the CFD simulation model

The mixing characteristics in the PBR play an important role in the production of the microalgae. Therefore, CFD simulation models were designed depending on the condition of the structural parameter (nozzle arrangement, the number of nozzles, baffle installation conditions, installation depth of the baffle, and bottom clearance) affecting the mixing characteristics in the PBR. In this case, the conditions of the structural parameters of the PBR were shown in the Table 5 and Fig. 16.

Table 5 Variables for the PBR design in CFD simulations

Variables	Conditions
Nozzle arrangement	1 line or 2 line zigzag
Number of nozzles	6, 10, and 12 EA
Baffle installation condition	with baffle and without baffle
Baffle installation depth	6.5, 13, and 19.5 cm
Bottom clearance	5, 10, 20, and 30 cm

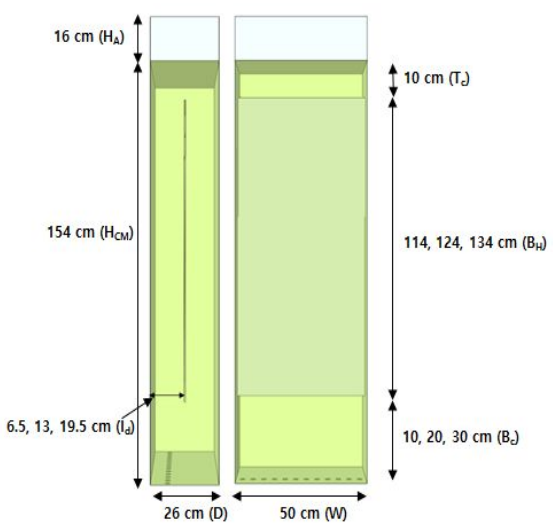

Fig. 16 Design information of Flat-plate PBR applied in this study

The grid size for the model design, the surface tension coefficient, and the

calculation time intervals have a significant effect on the results in performing a simulation study of each structural parameter of the PBR.

For the simulation calculation using the VOF model, it is necessary to carefully consider the value of the Courant number, which is updated at each calculation time interval in selecting grid size. The Courant number is the number of dimensionless calculation time intervals, grid size, and the difference in velocity (Eq. 14). It can evaluate the convergence for the interpretation area through the calculation time intervals, grid size, and velocity, etc., in the calculation process (Ansys CFD training manual, 2014).

$$\mathrm{CFL} = \frac{(\sum \lambda_f^{max} A_f \times \Delta t}{2V} \qquad \text{Eq. (14)}$$

Where,

Δt : Time step size

V : Cell volume

A_f : Face cell

λ_f^{max} : Eigenvalue

CFL : Courant number

Seo et al. (2012) deduced the correlation between the number of grids and grid sizes for a 20-L PBR in a range that does not exceed Courant number 250 in the calculation process and consequently suggested a 4 mm grid size as a suitable size considering an expandability of the simulation model later. Also, the surface tension in the simulation using the VOF model must be considered. The surface tension shows the pressure difference of the boundary surface between two phases in accordance with an angle that one phase formed in another phase, it was converted into the momentum, and calculated with the momentum equation of the governing equation of the VOF model. The injected bubble size was changed by the surface tension, and the larger bubble size increased the rising time of the

bubble since the resistance increased on the rise along with an increasing bubble size. Seo et al. (2012) experimented with the time required for the bubble to reach the surface of the water through the experiment and the estimated surface tension coefficient to show a similar CFD simulation result. In this study, the estimated surface tension coefficient was 0.048 N/m.

In general, the simulation model has been evaluated and suggests that the smaller the calculation time intervals, the higher the accuracy of the simulation; however, a computation time that was too small excessively increased the calculation time required to conduct the simulation, and the calculation time interval over a certain level led to an inaccuracy of value. Therefore, Seo et al. (2012) relatively compared the CFD simulation results with 0.001 sec of a calculation time interval, which is the smallest value, to determine the suitable calculation time interval of a multi-phase model. The simulation result is shown in Fig. 17. A distinct difference in the accuracy was confirmed in the case of exceeding a 0.005 sec of calculation time interval in terms of the time required for the initial bubble to reach the surface of the water. As a result, the calculation time interval 0.005 sec was selected for the accuracy of the simulation and the computing time.

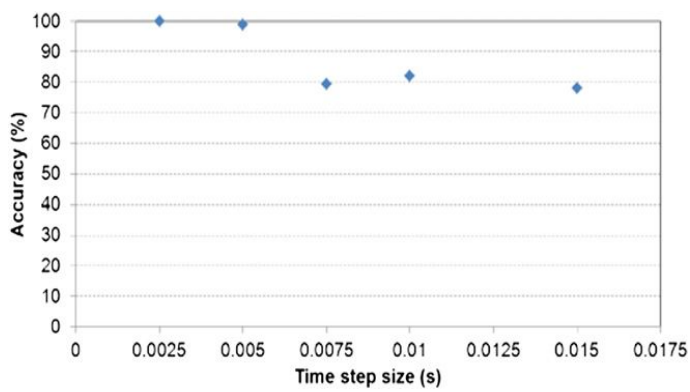

Fig. 17 Comparison of the CFD-computed difference of bubble rising time based on the initial bubble rising time of 0.001s (Seo et al., 2012)

Table 6 Input values for the target photobioreactor

Conditions	Values
Phase	Water(primary) / Air(secondary)
Turbulence model	Standard κ-ε
Multiphase model	Volume of Fluid
Time interval	0.005 s
Grid size	4 mm
Surface tension	0.048 N/m
Aeration rate	0.05 v/v/m

X, Y, and Z coordinate values for a minimum of 27,000~32,000 particles were extracted at regular calculation time interval according to the structural parameter based on the assumption that the microalgae in the PBR were uniformly distributed at the initiatory stage. The extracted coordinate value was used to calculate the distribution of light intensity for the depth from the Lambert-Beer's law. The calculated light intensity allowed for estimating the specific growth rate of the microalgae for the culture day. Lastly, the production of the microalgae for the culture day was calculated by using Eq. 15 in terms of the initial concentration of the microalgae 0.2 g/L and the light intensity 300 $\mu Em^{-2}s^{-1}$.

$$\mu = \frac{\ln(\frac{N_2}{N_1})}{t_2 - t_1} \qquad \text{Eq. (15)}$$

Where,

μ : Specific growth rate (day^{-1})

$N_{1,2}$: The number of cells/ml at the time

$t_{1,2}$: Time (day)

3.6.3. Statistical analysis for the simulation results

A two-way ANOVA can be used to investigate the changes of the dependent variables depending on the change level of two or more independent variables. Using this analysis, the main effect to investigate the effect on the dependent variable for the change of an independent variable can be analyzed. Additionally, the interaction effect on multiple effects between two or more independent variables can be conducted at the same time. In this study, the interaction effect was first analyzed according to each structural parameter of the photobioreactor using the two-way ANOVA. A general model of a two-way ANOVA can be written as:

$$Y_{ijk} = \mu + A_i + B_j + (AB)_{ij} + e_{ijk} \quad \text{Eq. (16)}$$

Where,

Y_{ijk} :

μ : The overall mean

A_i : i-th level of factor A

B_j : j-th level of factor B

AB_{ij} : The effect due to interaction between i-th level of factor A and j-th level of factor B

When the interaction effect did not show a significant difference, the one-way ANOVA was conducted to determine the main effect for each parameter; however, for indicating a significant difference, a Bonferroni post hoc test was conducted to determine the difference among the groups in detail. The result of the ANOVA table for factors A and B was shown in Table 7

Table 7 Calculation of a two-way ANOVA for factor A and B

Source	Sum of Square (SS)	df	Mean Square (MS)	F
Factor A	SS(A)	(a-1)	MSA=SS(A)/(a-1)	MSA/MSE
Factor B	SS(B)	(b-1)	MSB=SS(B)/(b-1)	MSB/MSE
Interaction AB	SS(AB)	(a-1)(b-1)	MSAB=SS(AB)/(a-1)(b-1)	MSAB/MSE
Error	SSE	(N-ab)	SSE/(N-ab)	
Corrected total		(N-1)		

4. Results and Discussion

4.1. Depth and height estimation of a flat-plate PBR

Seo et al. (2014) analyzed the concentration change of microalgae and compared culture experiments for 5 days with various microalgal growth models using a 20 L photobioreactor in the conditions of the initial concentration of microalgae of 0.2 g/L and a light intensity of 300 $\mu Em^{-2}s^{-1}$. The result of the culture experiment showed that it was similar to the growth model suggested by Steele (1977), as shown in Fig. 18.

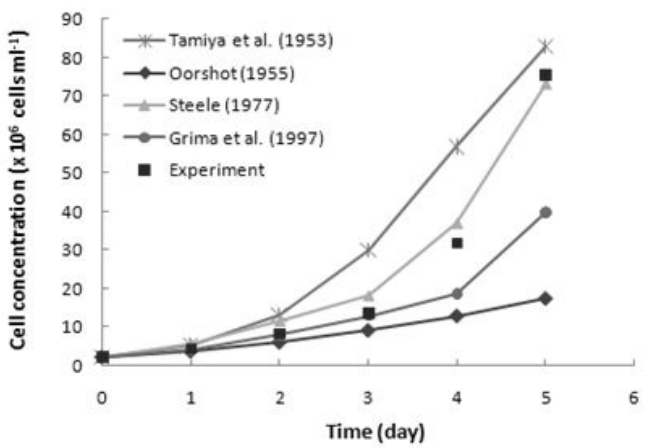

Fig. 18 Comparison between culture experimental and estimated data from four different growth model

The cell concentration of microalgae showed a decreasing trend under the condition of a light intensity below 250 $\mu Em^{-2}s^{-1}$ from the result of the cell concentration of the microalgae calculated in Steele's growth model in accordance with a light intensity from 100 to 350 $\mu Em^{-2}s^{-1}$. It was clearly revealed that a light intensity higher than 250 $\mu Em^{-2}s^{-1}$ was required to maintain the maximum specific growth rate (Fig. 19).

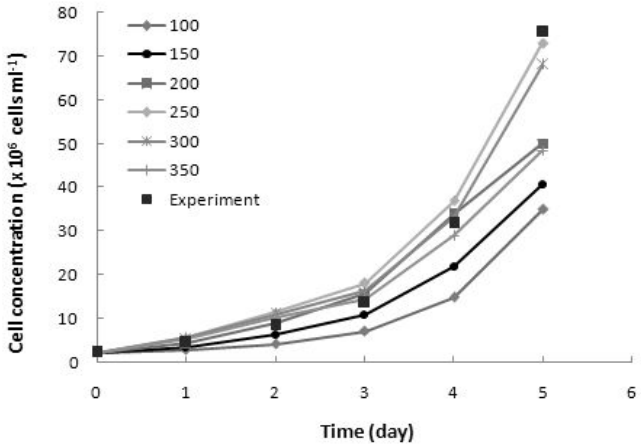

Fig. 19 Comparison of microalgal growth curve depending on the different light intensities

The depth from the illuminating surface of the light was able to maintain the light intensity of 250 $\mu Em^{-2}s^{-1}$ on the basis of a culture of 7 days, which was estimated using Lambert-Beer's law. The depth from the illuminating surface of the light up to 13 cm showed constant microalgae growth; however, the specific growth rate was identified to sharply decrease over 13 cm in depth.

Consequently, the depth of the PBR was designed to have 26 cm considering the unit productivity of the microalgae per culture, and the baffle was also installed in the light of the increased depth. Furthermore, 2 m was regarded as the maximum height when designing a PBR in reference to designing a standard relevant to a glass-covered greenhouse in Korea on the assumption that the PBR must be installed in a greenhouse because thermal screen, eaves height, and available space to maintain and harvest restricted the height applicable; however, a valid height was identified as 1.7 m considering an additional apparatus, such as a support beam and the space to install tubes for supplying CO_2 and O_2.

In this study, a proposed PBR with a unit module for enlargement was designed to be feasible to continuously and stably produce microalgae in the glass-covered greenhouse, the design dimension of the PBR was consisted of unit width

(50 cm), depth (26 cm), and height (170 cm). Fig. 20 schematically shows a proposed structural dimension.

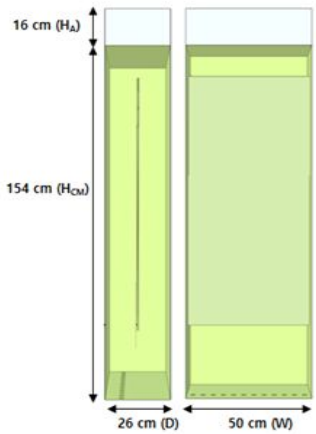

Fig. 20 Calculated outside structural dimension for a flat-plate PBR

4.2. Prediction of production from the simulation models

4.2.1. Pilot test results with regard to the top and bottom clearance of the PBR

The maximum production, which was predicted on the conditions that the top clearances were set to 10, 20, 30 cm, was 2.20 g/L while the minimum value was predicted at 2.10 g/L. The effect according to the top clearance on the predicted production showed only about 5 % difference, while the maximum and minimum production according to the bottom clearances showed 2.50 g/L and 1.95 g/L, respectively, the difference between two values was almost 28 %. From the result, a conclusion could be drawn that the bottom clearance could have a relatively greater influence on the microalgal production than the top clearance of the PBR. Therefore, the bottom clearance was selected as a parameter affecting the mixing characteristic inside the PBR, the top clearance was set to the 10 cm because a relatively distinct trend of the predicted production was shown.

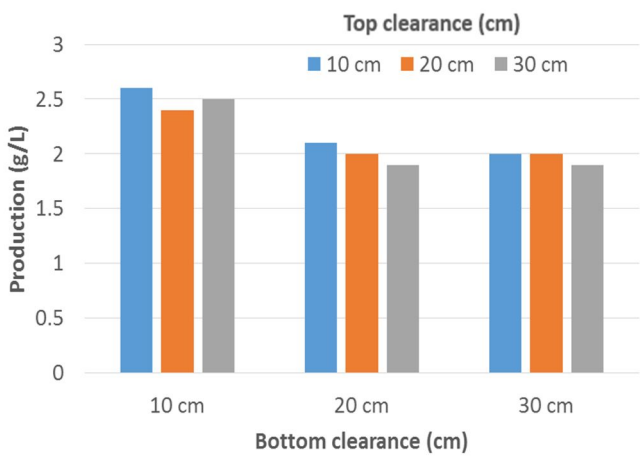

Fig. 21 The predicted production on the conditions between the top clearances (10, 20, 30 cm) and bottom clearances (10, 20, 30 cm) of the PBR

4.2.2. Production analysis with a baffle effect

The predicted production depended on the installation of a baffle inside the photobioreactor, which is illustrated in Table 8, and it showed a distinct difference. The production of the microalgae was identified to improve a minimum of 14%, a maximum of 90%, and an average of 41% of the production.

Table 8 Predicted average yields with 5 cm bottom clearance according to the installation of a baffle inside the PBR

Line arrangement (Line)	Number of nozzle (holes)	Nozzle location (cm)	Without baffle (g/L)	With baffle (g/L)	Rate of increase (%)
1	Six	6.5	3.01	4.60	53%
		13	2.32	2.87	24%
		19.5	1.63	2.26	39%
	Eight	6.5	3.17	4.62	46%
		13	2.27	2.92	29%
		19.5	1.62	1.84	14%
	Twelve	6.5	3.76	4.41	17%
		13	2.49	3.24	30%
		19.5	1.46	2.51	72%
2 (Zigzag)	Six	13	2.07	2.77	33%
		19.5	1.41	1.89	34%
	Eight	13	2.22	2.85	29%
		19.5	1.26	1.82	44%
	Twelve	13	2.10	3.58	71%
		19.5	1.32	2.50	90%

This occurred because with the installation of a baffle, the average light intensity the microalgae absorbed increased by 6%, and the homogeneity of the light was improved by 5%. Also, the installation of the baffle displayed a tendency

for increasing an improved effect of the light conditions with the passage of culture days (Table 9, Table 10). When the nozzle arrangement was in a 2-line zigzag arrangement, the number of nozzles was twelve holes, the baffle installation depth was 13 cm, and the bottom clearance was 5cm, a maximum of 29.7% of the light intensity was improved. As a result, the predicted production by CFD showed 2.10 g/L in the absence of installing the baffle, while the production increased by approximately 71% compared with the condition of installing the baffle (Fig. 22).

Table 9 Enhanced proportion of light absorption of the microalgae for culture day depending on the baffle installation conditions (the number of nozzle: twelve holes) (Unit: %)

Conditions		Day 1	Day 2	Day 3	Day 4	Day 5	Day 6	Day 7
1 Line nozzle & 6.5 cm baffle depth	No baffle vs. 5 cm	2.3	2.8	3.7	6.0	9.2	15.4	22.2
	No baffle vs. 10 cm	1.2	1.5	2.0	3.2	4.9	8.1	11.6
	No baffle vs. 20 cm	0.5	0.7	0.9	1.4	2.2	3.5	5.0
	No baffle vs. 30 cm	0.3	0.4	0.6	0.9	1.4	2.4	3.4
1 Line nozzle arrangement & 13 cm baffle depth	No baffle vs. 5 cm	3.4	4.1	5.5	8.5	12.8	20.1	27.1
	No baffle vs. 10 cm	1.2	1.4	1.8	2.7	3.8	5.1	5.5
	No baffle vs. 20 cm	-0.2	-0.3	-0.4	-0.8	-1.6	-3.6	-6.5
	No baffle vs. 30 cm	0.1	0.1	0.1	-0.1	-0.5	-2.0	-4.4
1 Line nozzle arrangement & 19.5 cm baffle depth	No baffle vs. 5 cm	1.8	2.2	2.9	4.3	6.1	8.3	9.1
	No baffle vs. 10 cm	1.1	1.4	1.7	2.4	3.1	3.2	2.0
	No baffle vs. 20 cm	0.8	1.0	1.2	1.7	2.1	2.0	0.8
	No baffle vs. 30 cm	0.6	0.8	0.9	1.2	1.2	0.3	-1.7

Table 10 Enhanced proportion of light absorption of the microalgae for culture day depending on the baffle installation conditions (the number of nozzle: twelve holes) (Unit: %)

Conditions		Day 1	Day 2	Day 3	Day 4	Day 5	Day 6	Day 7
2 Line zigzag arrangement & 13 cm baffle depth	No baffle vs. 5 cm	3.3	4.1	5.4	8.6	13.1	21.2	29.7
	No baffle vs. 10 cm	1.2	1.5	1.9	2.9	4.2	6.3	7.9
	No baffle vs. 20 cm	0.1	0.1	0.1	0.0	-0.2	-1.0	-2.3
	No baffle vs. 30 cm	-0.4	-0.4	-0.6	-1.0	-1.7	-3.1	-4.9
2 Line zigzag arrangement & 19.5 cm baffle depth	No baffle vs. 5 cm	2.8	3.4	4.5	6.7	9.6	13.7	16.8
	No baffle vs. 10 cm	2.5	3.0	3.9	5.9	8.4	12.1	14.8
	No baffle vs. 20 cm	1.1	1.3	1.6	2.3	3.0	3.7	3.9
	No baffle vs. 30 cm	1.1	1.3	1.6	2.2	2.8	3.2	2.7

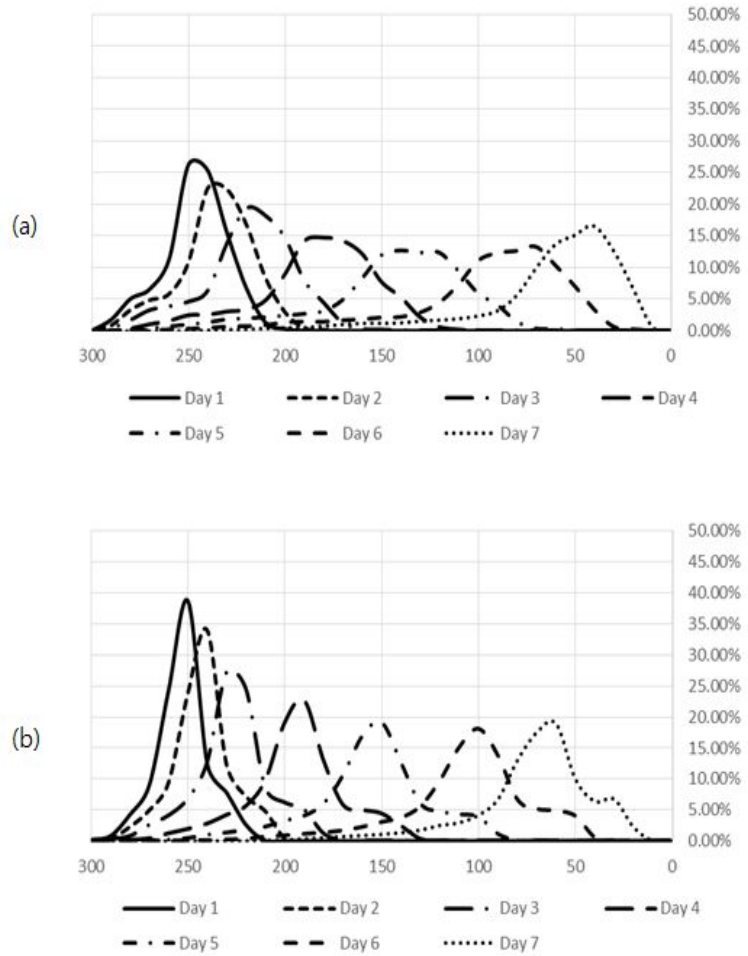

Fig. 22 Daily frequency for the light intensity absorbed from microalgae in the condition of installation of a baffle (a) PBR without baffle: 1 line, twelve nozzles, nozzle location 6.5 cm, (b) PBR with baffle: 1 line, twelve nozzles, nozzle location 6.5 cm, bottom clearance 5 cm

However, even though the production was enhanced in the condition of the bottom clearance of 5 cm, the other production depended on the bottom clearances of 10, 20, and 30 cm decreased. Consequently, the unconditional installation of the baffle did not have an improved effect on the production cultivated in the PBR (Table 11~Table 13). In other words, the suitable conditions of installing the baffle to improve the fluid flow characteristics inside the PBR was proposed to be significant since a volume of the riser and downcomer of the PBR or bottom

clearance can change the flow characteristics. Therefore, a preliminary feasibility study was considered to be required using a rheological characteristic according to the structural parameters, and the prediction model for the production, such as a BPMG model, should be used for an experimental or industrial PBR design.

Table 11 Predicted average yields with 10 cm bottom clearance according to the installation of a baffle inside the PBR

Line arrangement (Line)	Number of nozzle (holes)	Nozzle location (cm)	Without baffle (g/L)	With baffle (g/L)	Rate of increase (%)
1	Six	6.5	3.01	3.57	+19%
		13	2.32	2.06	-11%
		19.5	1.63	2.02	24%
	Eight	6.5	3.17	3.61	14%
		13	2.27	2.12	-7%
		19.5	1.62	1.66	2%
	Twelve	6.5	3.76	3.71	-1%
		13	2.49	2.66	7%
		19.5	1.46	2.09	43%
2 (Zigzag)	Six	13	2.07	2.05	-1%
		19.5	1.41	1.70	21%
	Eight	13	2.22	2.09	-6%
		19.5	1.26	1.53	21%
	Twelve	13	2.1	2.56	22%
		19.5	1.32	2.25	70%

Table 12 Predicted average yields with 20 cm bottom clearance according to the installation of a baffle inside the PBR

Line arrangement (Line)	Number of nozzle (holes)	Nozzle location (cm)	Without baffle (g/L)	With baffle (g/L)	Rate of increase (%)
1	Six	6.5	3.01	3.21	7%
		13	2.32	2.01	-13%
		19.5	1.63	1.55	-5%
	Eight	6.5	3.17	3.20	1%
		13	2.27	1.85	-19%
		19.5	1.62	1.32	-18%
	Twelve	6.5	3.76	3.53	-6%
		13	2.49	2.03	-19%
		19.5	1.46	1.81	24%
2 (Zigzag)	Six	13	2.07	1.99	-4%
		19.5	1.41	1.42	0
	Eight	13	2.22	1.93	-13%
		19.5	1.26	1.37	8%
	Twelve	13	2.1	2.08	-1%
		19.5	1.32	1.64	24%

Table 13 Predicted average yields with 30 cm bottom clearance according to the installation of a baffle inside the PBR

Line arrangement (Line)	Number of nozzle (holes)	Nozzle location (cm)	Without baffle (g/L)	With baffle (g/L)	Rate of increase (%)
1	Six	6.5	3.01	3.30	10%
		13	2.32	1.88	-19%
		19.5	1.63	1.44	-11%
	Eight	6.5	3.17	3.44	9%
		13	2.27	1.82	-20%
		19.5	1.62	1.32	-19%
	Twelve	6.5	3.76	3.55	-6%
		13	2.49	2.21	-11%
		19.5	1.46	1.72	18%
2 (Zigzag)	Six	13	2.07	1.82	-12%
		19.5	1.41	1.38	-2%
	Eight	13	2.22	1.93	-13%
		19.5	1.26	1.25	0
	Twelve	13	2.1	1.96	-6%
		19.5	1.32	1.57	19%

4.2.3. Production analysis with the installation depth of a baffle

Table 14 shows the predicted productions according to the installation depth of the baffle. The production when the baffle was located at 6.5 cm from the illuminating surface showed the highest production among different depths (13 and 19.5 cm) of the baffle at 3.73 g/L on the assumption that the light was illuminated into the PBR in one direction, as shown in Fig. 11. It also showed a tendency in

which the production was decreased by 38% and 24%, respectively, as the distance from the illuminated surface increased. When compared with the production between 6.5 cm and 13 cm of the installation depth of the baffle, it showed about 64% higher production because the light intensity and homogeneity were improved by an average of 4% and 2%, respectively. When compared with 19.5 cm, 112% of enhanced production was shown by an improvement of a 6% light intensity and 7% light homogeneity.

Table 14 Predicted average yield according to the installation depth of a baffle (g/L)

Installation depth	Mean	N	Std. deviation	Variance	Min	Max
6.5 cm	3.729	12	0.517	0.267	3.199	4.619
13 cm	2.304	24	0.498	0.248	1.816	3.581
19.5 cm	1.744	24	0.369	0.136	1.255	2.51

In particular, the predicted production of a 6.5 cm baffle installation depth based on the conditions in which eight nozzle holes were installed in a line and the bottom clearance was designed at 5 cm showed the highest at 4.62g/L, and the increase rate, which was approximately 60% higher than the production with a 19.5 cm baffle installation depth, was second highest at the same time. This is because the light intensity was enhanced by a maximum of 29%, and non-homogeneity was improved by 37% in comparison with a 19.5 cm baffle installation depth. In addition to the 13 cm baffle installation depth, the production was predicted to be 2.92 g/L, which was 37% higher than the production of a 19.5 cm baffle installation depth since it increased a maximum of 17% in light intensity and reduced by 50% in non-homogeneity (Table 15). When installing twelve nozzle holes in a line with a bottom clearance of 5 cm, the production was predicted as 4.41, 3.24, and 2.51 g/L depending on the baffle installation depth at 6.5, 13, and 19.5 cm, respectively. As a result, the larger the distance from the illuminating

surface rose, the more the predicted production decreased due to a reduction of 6% in light intensity and 7% in homogeneity. Fig. 22 shows the daily frequency of the light intensity absorbed from the microalgae between an installation depth of 6.5 cm and 19.5 cm in the same condition of twelve nozzle holes in a line and a 30 cm bottom clearance, and it showed a 50% production loss from an 11% reduction in the light intensity and an 82% increase in non-homogeneity.

Table 15 Predicted average yield according to the bottom clearance of a baffle when line arrangement was 1 line arrangement (g/L)

Number of nozzle (holes)	Bottom clearance (cm)	Installation depth of a baffle			Rate of increase (%)	
		6.5 cm	13 cm	19.5 cm	6.5 vs. 19.5 cm	13 vs. 19.5 cm
Six	5	4.60	2.87	2.26	51%	21%
	10	3.57	2.06	2.02	43%	2%
	20	3.21	2.01	1.55	52%	23%
	30	3.30	1.88	1.44	56%	23%
Eight	5	4.62	2.92	1.84	60%	37%
	10	3.61	2.12	1.66	54%	22%
	20	3.20	1.85	1.32	59%	28%
	30	3.44	1.82	1.32	62%	28%
Twelve	5	4.41	3.24	2.51	43%	23%
	10	3.71	2.66	2.09	44%	21%
	20	3.53	2.03	1.81	49%	11%
	30	3.55	2.21	1.72	52%	22%

There was a change in the amount of the predicted production in the conditions that 8 nozzle holes were installed in a 2-line zigzag arrangement and the bottom clearance was designed at 5 cm, which showed the highest at 36% similar with the production of a 1-line arrangement (Table 16). The highest production was shown for the conditions in which there were twelve nozzle holes and a 5 cm bottom clearance due to a relatively high efficiency on the average light intensity

for the microalgae to use at 186.4 $\mu Em^{-2}s^{-1}$ and its standard variation at just 7.4 $\mu Em^{-2}s^{-1}$.

Table 16 Predicted average yield according to the bottom clearance of a baffle when line arrangement was 2 line zigzag arrangement (g/L)

Number of nozzle (holes)	Bottom clearance (cm)	Installation depth of a baffle		Rate of increase (%)
		13 cm	19.5 cm	
Six	5	2.77	1.89	32%
	10	2.05	1.70	17%
	20	1.99	1.42	29%
	30	1.82	1.38	24%
Eight	5	2.85	1.82	36%
	10	2.09	1.53	27%
	20	1.93	1.37	29%
	30	1.93	1.25	35%
Twelve	5	3.58	2.50	30%
	10	2.56	2.25	12%
	20	2.08	1.64	21%
	30	1.96	1.57	20%

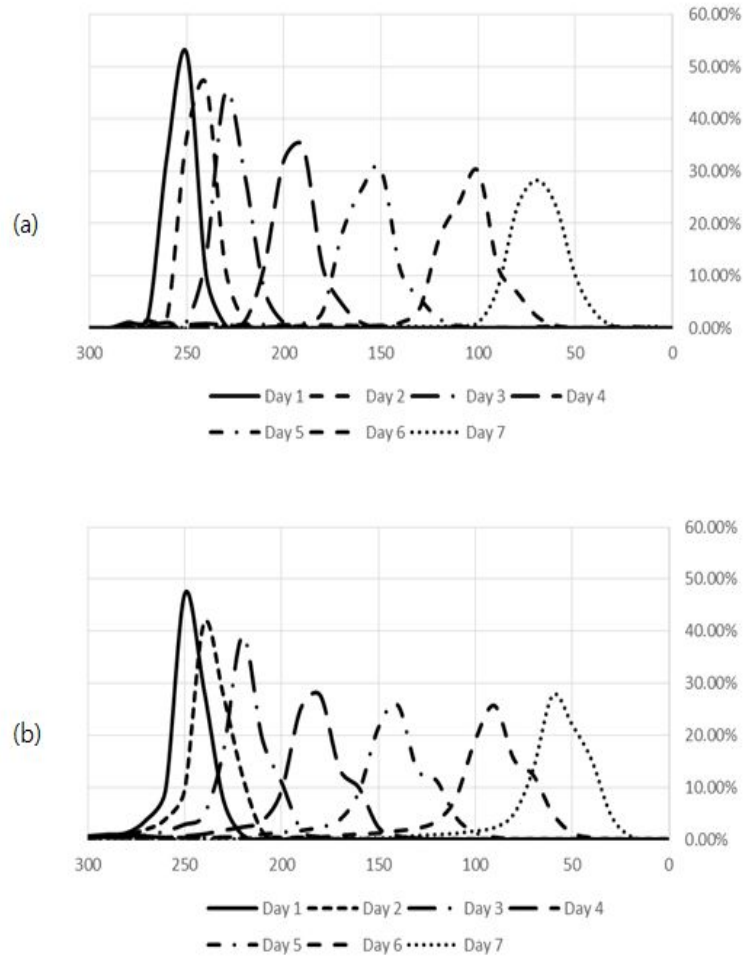

Fig. 23 Daily frequency for the light intensity absorbed from microalgae in the condition of the installation depth of a baffle (a) 1 line, twelve nozzles, bottom clearance 30 cm, and installation depth 6.5 cm, (b) 1 line, twelve nozzles, bottom clearance 30 cm, and installation depth 19.5 cm

4.2.4. Production analysis with the bottom clearance

The production analysis based on bottom clearance is listed in Table 17. The bottom clearance of 20 cm and 30 cm, which had the improvement effect of just 1%, did not show a distinct difference related to the production. The more the bottom clearance decreased, the more the predicted production increased. When comparing the bottom clearance of 5cm with 30 cm, an average of 47% production

was enhanced by increasing the average light intensity by 6% and the homogeneity of the light by 5% based on the result of the increase regarding the frequency of light exposure.

Table 17 Predicted average yield according to the bottom clearance of a baffle (g/L)

Bottom clearance	Mean	N	Std. deviation	Variance	Min	Max
5 cm	2.979	15	0.915	0.905	1.817	4.619
10 cm	2.379	15	0.7119	0.507	1.528	3.707
20 cm	2.062	15	0.696	0.484	1.324	3.529
30 cm	2.041	15	0.7687	0.591	1.255	3.55

Table 18 displays the production of the bottom clearances of 5, 10, 20, and 30 cm depending on the number of nozzles and the installation depth of the baffle when the nozzles were in a line. As mentioned, the bottom clearance of 5 cm has the highest production, and there was little difference in the production of under 8% between the bottom clearance of 20 cm and 30 cm. The highest value was similar with Yu et al. (2009), they mentioned that the optimal bottom clearance was in the rage of 2 ~ 6 cm, which was consistent with this study. Furthermore, Chisti (1989) announced that the influence of the bottom clearances on mixing between ranges mentioned above was not pronounced.

The highest production was shown at 4.62 g/L on the conditions that the 8 nozzle holes were installed in a line and the baffle installation depth was 6.5 cm. It had approximately 34% higher production compared with the bottom clearance of 30 cm because the light intensity was increased by a maximum of 20%, and the homogeneity of the light was improved by 12%. It also showed the highest increase rate on the same conditions compared with the bottom clearance of 5 cm and 30 cm because although the improvement of the homogeneity for the light was somewhat

low at 9 %, the light intensity was strongly enhanced by 24%.

Table 18 Predicted average yields with 1 line arrangement according to the bottom clearance of a baffle inside the PBR

Number of nozzle (holes)	Installation depth of a baffle	Bottom clearance of a baffle				Rate of increase between 5 cm and 30 cm (%)
		5 cm	10 cm	20 cm	30 cm	
Six	6.5 cm	4.60	3.57	3.21	3.30	39%
	13 cm	2.87	2.06	2.01	1.88	53%
	19.5 cm	2.26	2.02	1.55	1.44	57%
Eight	6.5 cm	4.62	3.61	3.20	3.44	34%
	13 cm	2.92	2.12	1.85	1.82	61%
	19.5 cm	1.84	1.66	1.32	1.32	40%
Twelve	6.5 cm	4.41	3.71	3.53	3.55	24%
	13 cm	3.24	2.66	2.03	2.21	46%
	19.5 cm	2.51	2.09	1.81	1.72	46%

Table 19 displays the production of bottom clearances of 5, 10, 20, and 30 cm depending on the number of nozzles and the installation depth of the baffle when the nozzles were in a 2-line zigzag arrangement. As mentioned, the bottom clearance of 5 cm had the highest production, and there was little difference in the production under 10% between the bottom clearances of 20 cm and 30 cm.

The highest production was shown at 3.58 g/L on the conditions that the 8 nozzle holes were installed in a 2-line zigzag arrangement and the baffle installation depth was 13 cm. It had the highest increase rate at the same time and approximately an 82% higher production compared with the bottom clearance of 30 cm. This is because the light intensity was only improved by 14%, while the homogeneity was improved by 59%.

Table 19 Predicted average yields with 2 line zigzag arrangement according to the bottom clearance of a baffle inside the PBR

Number of nozzle (holes)	Installation depth of a baffle	Bottom clearance of a baffle				Rate of increase (%)
		5 cm	10 cm	20 cm	30 cm	
Six	13 cm	2.77	2.05	1.99	1.82	52%
	19.5 cm	1.89	1.70	1.42	1.38	37%
Eight	13 cm	2.85	2.09	1.93	1.93	48%
	19.5 cm	1.82	1.53	1.37	1.25	45%
Twelve	13 cm	3.58	2.56	2.08	1.96	82%
	19.5 cm	2.50	2.25	1.64	1.57	60%

In addition, the production with twelve nozzle holes in a line and an installation depth of 19.5 cm was compared in accordance with the bottom clearances. The results are shown in Table 20, and the production was confirmed to have 2.51, 2.09, 1.81, and 1.72 g/L with bottom clearances of 5, 10, 20, and 30 cm, respectively. When comparing the bottom clearance of 5 cm with 30 cm, an improvement efficiency of an average of 41% was identified by improving the light intensity by 5% and the homogeneity by 3% due to an increased frequency of light exposure.

Table 20 Predicted yields depending on the bottom clearances of a baffle

Baffle bottom clearance	Yield
-	1.46 g/L
5 cm	2.51 g/L
10 cm	2.09 g/L
20 cm	1.81 g/L
30 cm	1.72 g/L

Moreover, a comparison result between bottom clearances of 5 cm and 30 cm with the same conditions of twelve nozzle holes in a 2-line zigzag and a baffle installation depth of 19.5 cm resulted in each production being 2.50 g/L and 1.57 g/L, respectively. The production was decreased by 34% by increasing the bottom clearance because the light intensity of 12% was decreased and its non-homogeneity of 9% was increased (Fig. 23).

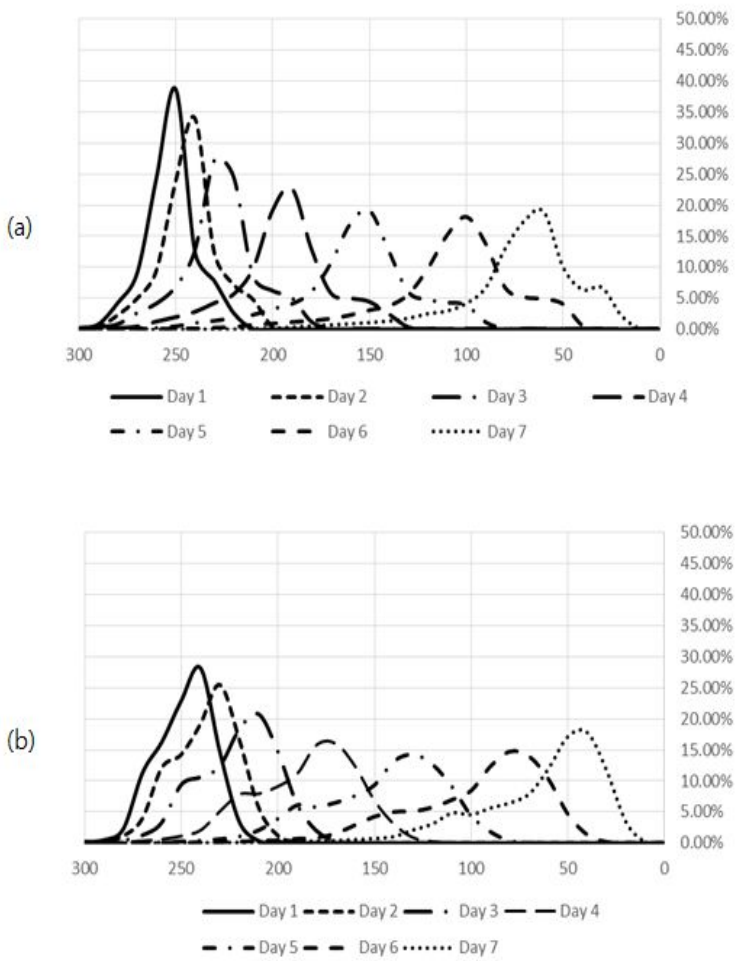

Fig. 24 Daily frequency for the light intensity absorbed from microalgae in the condition of the installation depth of a baffle (a) 2 line, twelve nozzles, installation depth 19.5 cm, and bottom clearance 5 cm (b) 2 line, twelve nozzles, installation depth 19.5 cm, and bottom clearance 30 cm

4.2.5. Production analysis with the number of nozzles

Table 21 displays the predicted productions with the number of nozzles. When the number of nozzles was six, eight, and twelve holes, the productions expected to show 2.29, 2.22, and 2.58 g/L, respectively, based on the assumption of injecting the same amount of mixing gas (CO_2 and O_2). From the results, a 3% difference was identified when comparing 6 with 8 nozzle holes. It can be concluded that there was little difference in the production; however, the average production with twelve nozzle holes was 16% higher on average since it had a relatively higher light intensity of 4% and homogeneity of 3% on average.

Table 21 Predicted average yields depending on the number of nozzles

Number of nozzle	Mean	N	Std. deviation	Variance	Min	Max
6	2.29	20	0.843	0.71	1.379	4.599
8	2.224	20	0.915	0.838	1.255	4.619
12	2.581	20	0.814	0.662	1.566	4.41

The production based on the number of nozzles on the conditions of bottom clearances of 5, 10, 20, and 30 cm when the installation depth was 6.5 cm and the nozzle arrangement was 1 line is shown in Table 22.

Most of the models with twelve nozzle holes showed higher production than the others; however, the increase rate of the production on the condition of the baffle installation depth of 6.5 cm became a single digit. In particular, the production with a bottom clearance of 5 cm and eight nozzle holes showed the highest value with an increase rate of 5% compared with the minimum production by enhancing the light intensity by 10%, although the homogeneity was reduced by 3%.

Table 22 Predicted average yields with 6.5 cm installation depth of a baffle according to the bottom clearance of a baffle inside the PBR (1 line arrangement)

Bottom clearance	The number of nozzles			Rate of increase between min and max (%)
	six holes	eight holes	twelve holes	
5 cm	4.60	4.62	4.41	5%
10 cm	3.57	3.61	3.71	4%
20 cm	3.21	3.20	3.53	10%
30 cm	3.30	3.44	3.55	7%

The production with the number of nozzles on the conditions of bottom clearance of 5, 10, 20, and 30 cm when the installation depth was 13 cm and the nozzle arrangement was 1 line is listed in Table 23. All of the models with twelve nozzle holes showed the highest production regardless of bottom clearances. There was an increase rate of 18% on average when comparing the maximum with minimum production. In particular, the production with six nozzle holes showed the lowest production, and twelve nozzle holes had a 29% higher production compared to six nozzle holes due to enhancing the light intensity by 12% and improving the homogeneity by 8% at the same time.

Table 23 Predicted average yields with 13 cm installation depth of a baffle according to the bottom clearance of a baffle inside the PBR (1 line arrangement)

Bottom clearance	The number of nozzles			Rate of increase between min and max (%)
	six holes	eight holes	twelve holes	
5 cm	2.87	2.92	3.24	13%
10 cm	2.06	2.12	2.66	29%

20 cm	2.01	1.85	2.03	10%
30 cm	1.88	1.82	2.21	22%

The production with the number of nozzles on the conditions of bottom clearances of 5, 10, 20, and 30 cm when the installation depth was 19.5 cm and the nozzle arrangement was 1 line is listed in Table 24. All of the models with twelve nozzle holes showed the highest production regardless of the bottom clearances equal to the baffle installation depth of 13 cm, while all the models with eight nozzle holes showed the lowest. The production of twelve nozzle holes was considered to have an improved production of 32% on average in comparison to the eight nozzle holes. The production with a bottom clearance of 5 cm and twelve nozzle holes showed the highest value in comparison to eight nozzle holes due to an increasing light intensity of 8% and decreasing non-homogeneity of 7%.

Table 24 Predicted average yields with 19.5 cm installation depth of a baffle according to the bottom clearance of a baffle inside the PBR (1 line arrangement)

Bottom clearance	The number of nozzles			Rate of increase between min and max (%)
	six holes	eight holes	twelve holes	
5 cm	2.26	1.84	2.51	37%
10 cm	2.02	1.66	2.09	26%
20 cm	1.55	1.32	1.81	37%
30 cm	1.44	1.32	1.72	31%

Table 25 shows the production with the number of nozzles on the conditions of 5, 10, 20, and 30 cm when nozzles were in a 2-line zigzag arrangement and the baffle installation depth was 13 cm. All of the models with twelve nozzle holes showed the highest production regardless of the bottom clearances with an increase rate of 17% on average when comparing the maximum with the minimum

production. Notably, an increased rate with the bottom clearances of 20 and 30 cm showed a mere 8 % on average, but an average of a 27% increase rate was shown with bottom clearances of 5 and 10 cm. In addition, twelve nozzle holes with a bottom clearance of 5 cm showed the highest production, which was 29% higher than six nozzle holes. This is because the light intensity was increased by 8%, and the homogeneity of the light was improved by 4%.

Table 25 Predicted average yields with 13 cm installation depth of a baffle according to the bottom clearance of a baffle inside the PBR (2 line zigzag arrangement)

Bottom clearance	The number of nozzles			Rate of increase between min and max (%)
	six holes	eight holes	twelve holes	
5 cm	2.77	2.85	3.58	29%
10 cm	2.05	2.09	2.56	25%
20 cm	1.99	1.93	2.08	8%
30 cm	1.82	1.93	1.96	8%

Table 26 shows the production with the number of nozzles on the conditions of 5, 10, 20, and 30 cm when the nozzles were in a 2-line zigzag arrangement and the baffle installation depth was 19.5 cm. All of the models with twelve nozzle holes showed the highest production, which is similar with other models. It had the same tendency as the model that consisted of a baffle installation depth of 13 cm and a 1-line arrangement. There was an increase in the rate of 32% on average when comparing the maximum with the minimum production. Notably, an increase rate at the bottom clearance of 10 cm with twelve nozzle holes showed the highest production, which was 47% higher than eight nozzle holes due to an increased light intensity of 15% and an increased homogeneity of the light by 7%.

Table 26 Predicted average yields with 19.5 cm installation depth of a baffle according to the bottom clearance of a baffle inside the PBR (nozzle arrangement: 2 line zigzag)

Bottom clearance	The number of nozzles			Rate of increase between min and max (%)
	six holes	eight holes	twelve holes	
5 cm	1.89	1.82	2.50	38%
10 cm	1.70	1.53	2.25	47%
20 cm	1.42	1.37	1.64	20%
30 cm	1.38	1.25	1.57	25%

4.2.6. Production analysis with the nozzle arrangement

Table 27 shows the analyzed production in accordance with the nozzle arrangement reflecting the number of nozzles, as mentioned previously. The production was predicted to have 2.61 g/L and 2.00 g/L, respectively, depending on the 1-line or 2-line zigzag arrangement due to an increased light intensity of 5.4% and a simultaneous improvement in the light homogeneity of 14.8%.

Table 27 Predicted average production depending on the nozzle arrangements

Line arrangement	Mean	N	Std. deviation	Variance	Min	Max
1	2.61	36	0.94	0.89	1.317	4.619
2 (Zigzag)	1.997	24	0.55	0.299	1.255	3.581

When there were 6 nozzle holes, a baffle installation depth of 13 cm, and bottom clearances of 5, 10, 20, and 30 cm, the production in accordance with the nozzle arrangement showed the production of a 1-line arrangement to be almost 3% higher than a 2-line zigzag arrangement. In particular, an improvement efficiency of a maximum of 4% on the condition of a bottom clearance of 5 cm caused the difference according to the condition of the arrangement to be small (Table 28). This is because the light intensity for the microalgae to absorb was enhanced by only 1%.

Table 28 Predicted average yields with 13 cm installation depth of a baffle according to the bottom clearance of a baffle inside the PBR (number of nozzle: six holes)

Bottom clearance	Line arrangement		Rate of increase between min and max (%)
	1 line	2 line (Zigzag)	
5 cm	2.87	2.77	4%
10 cm	2.06	2.05	1%
20 cm	2.0	1.99	1%
30 cm	1.88	1.82	3%

In addition, less than a 10% of increase in the rate of production when comparing a 1-line arrangement with a 2-line zigzag arrangement was shown, and the decreasing tendency of production occurred according to some of the installation conditions; however, when the number of nozzles was 6 holes, the baffle installation depth was 19.5 cm, and the bottom clearances were 5, 10, 20, and 30 cm, an improvement of an average of 13% in the production according to the nozzle arrangement was confirmed.

In particular, when six nozzle holes were installed in a line with a baffle installation depth of 19.5 cm and a bottom clearance of 5 cm, the production of

2.26 g/L was predicted for a 1-line arrangement, and the production was approximately 20% higher than the production (1.88 g/L) of a 2-line zigzag arrangement. This is because although the light intensity was enhanced by 0.5%, the homogeneity was increased by 8.9%. The rest of production rates according to the arrangement and the baffle installation depth on the same conditions are listed in Table 29~Table 33.

Table 29 Predicted average yields with 19.5 cm installation depth of a baffle according to the bottom clearance of a baffle inside the PBR (number of nozzle: six holes)

Bottom clearance	Line arrangement		Rate of increase between min and max (%)
	1 line	2 line (Zigzag)	
5 cm	2.26	1.89	20%
10 cm	2.02	1.70	19%
20 cm	1.55	1.42	10%
30 cm	1.44	1.38	5%

Table 30 Predicted average yields with 13 cm installation depth of a baffle according to the bottom clearance of a baffle inside the PBR (number of nozzle: eight holes)

Bottom clearance	Line arrangement		Rate of increase between min and max (%)
	1 line	2 line (Zigzag)	
5 cm	2.92	2.85	2%
10 cm	2.12	2.09	1%
20 cm	1.85	1.93	-4%
30 cm	1.82	1.93	-6%

Table 31 Predicted average yields with 19.5 cm installation depth of a baffle according to the bottom clearance of a baffle inside the PBR (number of nozzle: eight holes)

Bottom clearance	Line arrangement		Rate of increase between min and max (%)
	1 line	2 line (Zigzag)	
5 cm	1.84	1.82	1%
10 cm	1.66	1.53	9%
20 cm	1.32	1.37	-3%
30 cm	1.32	1.25	5%

Table 32 Predicted average yields with 19.5 cm installation depth of a baffle according to the bottom clearance of a baffle inside the PBR (number of nozzle: twelve holes)

Bottom clearance	Line arrangement		Rate of increase between min and max (%)
	1 line	2 line (Zigzag)	
5 cm	2.51	2.50	0
10 cm	2.09	2.25	-7%
20 cm	1.81	1.64	11%
30 cm	1.72	1.57	10%

Table 33 Predicted average yields with 13 cm installation depth of a baffle according to the bottom clearance of a baffle inside the PBR (number of nozzle: twelve holes)

Bottom clearance	Line arrangement		Rate of increase between min and max (%)
	1 line	2 line (Zigzag)	
5 cm	3.24	3.58	-9%
10 cm	2.66	2.56	4%
20 cm	2.03	2.08	3%
30 cm	2.21	1.96	13%

4.3. Statistical analysis of structural parameters

Table 34 showed the effect of the interactions among the three parameters of the number of nozzles, the depth of the baffle installation, and the bottom clearance. The nozzles arrangement was excluded from the analysis because it had a low power of explanation about own variable. There was no effect of the interaction at the significance level $p<.05$ with $F=.177$ for the interaction of the number of nozzles, the baffle installation depth, and the bottom clearance. That is, there was no interaction effect among the number of nozzles, the baffle installation depth, and the bottom clearance on the productivity of the microalgae. In addition, there was no difference in the effect of the interaction at the significance level $p<.05$ with $F=.177$ between the number of nozzles and the baffle installation depth. There was also no difference for the effect of the interaction at the significance level $p<.05$ with $F=.041$ between the number of nozzles and the bottom clearance for the baffle. A difference was found at the significance level $p<.05$ with $F=1.19$ between the baffle installation depth and the bottom clearance, and the interaction between the baffle installation depth and the bottom clearance on the design of the photobioreactor was thought to be significant.

Table 34 Analysis of interaction effect among the structural parameters for PBR

Source	Sum of Squares	df	Mean Square	F	Sig.
Correction model	34.639(a)	35	.990	2.702	.007
Intercept	314.542	1	314.542	858.812	.000
Number of nozzles	1.062	2	.531	1.450	.254
Installation depth	23.246	2	11.623	31.736***	.000
Bottom clearance	13.252	3	4.417	12.060***	.000
Number of nozzles * Installation depth	.259	4	.065	.177	.948
Number of nozzles * Bottom clearance	0.091	6	.015	.041	1.000
Installation depth * Bottom clearance	2.620	6	.437	1.192	.034
Number of nozzles * Installation depth * Bottom clearance	.266	12	.022	.061	1.000
Error	8.790	24	.366		
Total	378.975	60			
Corrected total	43.429	59			

* p<.05, ** p<.01, *** p<.001

The results of the analysis of the main effect among the number of nozzles, the baffle installation depth, and the bottom clearance are shown in Table 35. The baffle installation depth (F=31.73) and the bottom clearance for the baffle (F=12.06), with the exception of the number of nozzles, was shown to be significant at the significance level p<.001. The Bonferroni post hoc test was used to investigate the results in detail, and all installation depths (6.5, 13, 19.5 cm) were shown to be meaningful (Table 36).

Table 35 Verification of main effect by Bonferroni

		Sum of Squares	df	Mean Square	F	Sig.
Number of nozzles	Contrast	1.062	2	.531	1.450	.254
	Error	8.790	24	.366		
Installation depth	Contrast	23.246	2	11.623	31.736***	.000
	Error	8.790	24	.366		
Bottom clearance	Contrast	13.252	3	4.417	12.060***	.000
	Error	8.790	24	.366		

* p<.05, ** p<.01, *** p<.001

There was a meaningful difference between a 5 cm bottom clearance and a 20 cm and 30 cm bottom clearance (p<.01). While there was not a meaningful difference in the case of a 10 cm bottom clearance, a 20 cm bottom clearance showed a meaningful difference with a 5 cm bottom clearance, and a 30 cm bottom clearance also showed a meaningful difference with a 5 cm bottom clearance (p<.01).

Table 36 Bonferroni post hoc test

	(I)	(J)	Mean difference (I-J)	Std. Error	Sig.	95% Confidence interval	
						Lower bound	Upper bound
Number of nozzles	6	8	.0650	.19138	1.000	-.4275	.5575
		12	-.2910	.19138	.424	-.7835	.2015
	8	6	-.0650	.19138	1.000	-.5575	.4275
		12	-.3560	.19138	.225	-.8485	.1365
	12	6	.2910	.19138	.424	-.2015	.7835
		8	.3560	.19138	.225	-.1365	.8485
Installation depth	6.5	13	.5942*	.20459	.023	.0676	1.1207
		19.5	1.2820***	.18083	.000	.8166	1.7474
	13	6.5	-.5942*	.20459	.023	-1.1207	-.0676
		19.5	.6878**	.19919	.006	.1752	1.2005
	19.5	6.5	-1.2820***	.18083	.000	-1.7474	-.8166
		13	-.6878**	.19919	.006	-1.2005	-.1752
		10	.6000	.22098	.072	-.0353	1.2353
		5	.9160**	.22098	.002	.2807	1.5513
		20	.9393**	.22098	.002	.3040	1.5747
Bottom clearance	10	5	-.6000	.22098	.072	-1.2353	.0353
		20	.3160	.22098	.994	-.3193	.9513
		30	.3393	.22098	.826	-.2960	.9747
	20	5	-.9160**	.22098	.002	-1.5513	-.2807
		10	-.3160	.22098	.994	-.9513	.3193
		30	.0233	.22098	1.000	-.6120	.6587
	30	5	-.9393**	.22098	.002	-1.5747	-.3040
		10	-.3393	.22098	.826	-.9747	.2960
		20	-.0233	.22098	1.000	-.6587	.6120

* p<.05, ** p<.01, *** p<.001

These results were re-verified through a moderated regression analysis. Table 37 shows the results of the statistical analysis of the nozzle arrangement, the number of nozzles, the baffle installation depth, and the bottom clearance. The adjusted R-square was 0.600, showing a 60% power of the explanation regarding the statistical regression model of microalgal production according to each structural parameter calculated by a simulation prediction model (Table 38).

The impact factor of the structural parameter on the microalgae production was relatively compared. First, the nozzle arrangement was excluded due to the problem of multicollinearity. VIF (Variable Inflation Factor) and tolerance were investigated to determine the multicollinearity among the final parameters. Generally, there is a problem with multicollinearity when the variable inflation factor is larger than 10 or the tolerance is less than 0.1. In this study, the problem with multicollinearity did not occur because the VIF value of all of the parameters was less than 10, and the tolerance was larger than 0.1.

Table 37 Summary of model for moderated regression analysis

Model	R	R-square	Adjust R-square	Std. Error of the estimate
1	.798(a)	.636	.617	.53107
2	.798(b)	.637	.611	.53520
3	.799(c)	.638	.605	.53924
4	.804(d)	.646	.606	.53825
5	.805(e)	.647	.600	.54275

Table 38 Summary of model for moderated regression analysis

Model		Sum of Squares	df	Mean Square	F	Sig.
1	Regression	27.635	3	9.212	32.661***	.000
	Residual	15.794	56	.282		
	Total	43.429	59			
2	Regression	27.675	4	6.919	24.155***	.000
	Residual	15.754	55	.286		
	Total	43.429	59			
3	Regression	27.727	5	5.545	19.071***	.000
	Residual	15.702	54	.291		
	Total	43.429	59			
4	Regression	28.074	6	4.679	16.151***	.000
	Residual	15.355	53	.290		
	Total	43.429	59			
5	Regression	28.111	7	4.016	13.633***	.000
	Residual	15.318	52	.295		
	Total	43.429	59			

* p<.05, ** p<.01, *** p<.001

The analyzed results affecting the production of the microalgae with each structural parameter are shown in Table 39. The number of nozzles had β=.159 and did not have a meaningful impact on the significance level p<.05. The installation depth showed a negative meaningful impact of β=-.681 (p<.001). The bottom clearance also appeared to have a negative meaningful impact of β=-.432 (p<.001).

That is, the order of the impact on the production for the microalgae was shown as follows: 1) the baffle installation depth (-8.437***), 2) the bottom

clearance of baffle (-5.346***), and 3) the number of nozzles (1.975) (Table 39).

Table 39 Predicted production by moderated regression analysis

	Model 1			Model 2			Model 3			Model 4			Model 5		
	Beta	t	Sig.	Beta	t	Sig.	Beta	t	Sig.	Beta	t	Sig.	Beta	t	Sig.
(Constant)		12.060	.000		6.261	.000		4.900	.000		4.974	.000		3.356	.001
Number of nozzles	.159	1.975	.053	.087	.417	.679	.151	.583	.562	.151	.584	.562	.023	.051	.960
Installation depth	-.681	-8.437***	.000	-.787	-2.680**	.010	-.779	-2.627*	.011	-.941	-2.843	.006	-1.125	-1.82	.074
Bottom clearance	-.432	-5.346***	.000	-.432	-5.305***	.000	-.311	-1.050	.299	-.530	-1.484	.144	-.777	-.987	.328
Number of nozzles * installation depth				.131	.374	.710	.121	.342	.734	.121	.343	.733	.350	.473	.638
Number of nozzles * bottom clearance							-.139	-.423	.674	-.139	-.424	.673	.146	.167	.868
Installation depth * bottom clearance										.278	1.095	.279	.593	.640	.525
Number of nozzles * installation depth * bottom clearance													-.348	-.353	.725

* p<.05, ** p<.01, *** p<.001

5. Conclusion

In this study, the design dimension of the PBR was first estimated to be able to sustain the maximum specific growth rate. Then, the production of microalgae on the conditions of structural parameters was analyzed in the design of a photobioreactor using computational fluid dynamics. Next, the main and interaction effect were investigated to suggest the order of the priority of structural parameters in the design of the PBR.

A suitable design dimension was estimate to be able to make the best use of light efficiency in consideration of decreasing light penetration depth depending on culture days on the assumption that the PBR with unit module was installed in a greenhouse. The estimated dimension of the PBR was consisted of 50 cm in width, 26 cm in depth, and 170 cm in height.

The installation of the baffle to improve the inner flow characteristics in the design of the PBR enhanced production by an average of 40% because the average light intensity and homogeneity of the light that the microalgae absorbed were improved; however, an unconditional installation of the baffle in the PBR did not have a positive effect on the production of microalgae, so a proper consideration of the installation depth and the bottom clearance of the baffle was necessary.

A result of analyzing the effect of the installation depth of the baffle showed that the closer the baffle was installed from the surface of light penetration, the higher the production increased. A 13 cm and 19.5 cm installation depth compared with a 6.5 cm installation depth of the baffle decreased the production by 38% and 24%, respectively, because the larger the distance from the surface the light penetration increased, the more the average light intensity for the microalgae to absorb decreased.

Bottom clearance showed a decreasing trend of the microalgae by increasing the bottom clearance. The highest production, an average of 2.98 g/L, was shown in the bottom clearance of 5 cm. This was approximately a 46% increase in the

production compared with the production of the bottom clearance of 30 cm. Although there was no distinct trend for production in accordance with a change in the number of nozzles, there was an average of a 16% increase in the production in the case of installing twelve nozzles. When a 1-line arrangement of the nozzles was installed, the production with a 2-line zigzag arrangement of the nozzle was enhanced by 30%.

The interaction effect between the installation depth and the bottom clearance of the baffle showed a significant difference in the confidence interval at 95%, but the other interactions of the structural parameters did not show significant difference. The installation depth and the bottom clearance of the baffle showed a significance in the confidence level of 99.9% on the basis of the Bonferroni post hoc test for the result of the main effect. In addition, the relative influence of the structural parameters chosen for production was evaluated in order. The installation of the baffle (-8.437^{***}), the bottom clearance of the baffle (-5.346^{***}), and the number of nozzles (1.975) in order showed a higher influence compared with t-values.

Bibliography

Ahn, D. G., C. G. Cho, S. H. Jeong, and D. G. Lee. 2011. Design of photobioreactor for mass production of microalgae. *Journal of the korean society for precision engineering*. 28(2), 140-153.

Anna, J., C. B. Ethel, G. S. Karl, H. Peter, O. Rainer, J. H. Michael, Z. Nikolaos and P. Clemens. 2012. The application of transparent glass sponges for improvement of light distribution in photobioreators. *Journal of bioprocessing and biotechniques*. 2(1), 1-8.

Barbosa, M. J., M. Albrecht, and R. H. Wijffels, 2003. Hydrodynamic stress and lethal events in sparged microalgae cultures. *Journal of Biorechnology and Bioengineering*. 83, 112-120.

Bari, G. S., S. P. Gent, T. N. Suess, and G. A. Anderson, 2012. Hydrodynamic and heat transfer effects of different sparger spacings within a column photobioreactor using computational fluid dynamics. *ASME 2012 International Mechanical Engineering Congress and Exposition.*

Bitog, J. P. P., I. B. Lee, C. G. Lee, K. S. Kim, H. S. Hwang, S. W. Hong, I. H. Seo, K. S. Kwon, and E. Mostafa. 2011. Application of computational fluid dynamics for modeling and designing photobioreactors for microalgae production: A review. *Journal of Computers and Electronics in Agriculture*. 76, 131-147.

Bitog, J. P. P., I. B. Lee, H. M. Oh, S. W. Hong, I. H. Seo, and K. S. Kwon, 2014. Optimised hydrodynamic parameters for the design of photobioreactors using computational fluid dynamics and experimental validation. *Journal of Biosystems Engineering*. 122, 42-61.

Contreras, A., F. Garcia, E. Molina, J. C. Merchuk, 1998. Interaction between CO_2-mass transfer, light availability, and hydrodynamic stress in the growth of

phaeodactylum trcornutum in a concentric tube airlift photobioreactor. *Journal of Biotechnology and bioengineering*. 60(3), 317-325.

Couveryt, A., Roustan, M., Chatellier, P., 1999. Two-phase hydrodynamic study of a rectangular air-lift loop reactor with an internal baffle. *Journal of chemical engineering science*. 54, 5245-5252.

Chisti, Y., 2007. Biodiesel from microalgae. *Journal of Biotechnology Advances*. 25, 294-306.

Choi, H. J and S. M, Lee, 2011. Effect of temperature, light intensity and pH on the growth rate of *chlorella vulgaris*. *Journal of Korean Society of Environmental Engineering*. 33, 511-515.

Deckwer, W. D. 1992. Bubble column reactors. Chichester, UK; John wiley & Sons. .

Degen, J., A. Uebele, A. Retze, U. Schmid-staiger, W. Trosch, 2001. A novel airlift photobioreactor with baffles for improved light utilization through the flashing light effect. *Journal of Biotechnology*. 92(2), 89-94.

Fabregas, J., A. Dominguez, M. Regueiro, A. Maseda, and A. Otero, 2000. Optimization of culture medium for the continuous cultivation of the microalga *haematococcus pluvialis*. *Journal of applied microbiological biotechnol*. 53, 530-535.

Food and Agriculture Organization of the united nation (FAO), 2004. Hatcher culture of bivalves: A practical manual, http://www.fao.org/

Huang, J., F. Feng, M. Wan, J. Ying, Y. Li, X. Qu, R. Pan, G. Shen, W. Li. Improving performance of flat-plate photobioreactors by installation of novel internal mixers optimized with computational fluid dynamics. Journal of Bioresource Technology. 182, 151-159.

Huang, J., S. Kang, M. Wan, Y. Li, X. Qu, F. Feng, J. Wang, W. Wang, G. Shen, W. Li. 2015. Numerical and experimental study on the performance of flat-plate photobioractors with different inner structures for microalgae cultivation. *Journal of applied phycology*. 27, 39-58.

International Energy Agency (IEA). 2011. Http://www.iea.org.

Janvanmardian, M., and Palsson, B. O. 1991. High density photoautotrphic algal cultures: design, construction and operation of a novel photobioreactor system. *Journal of biotechnology and bioengineering*. 38, 1182-1189.

Jhawar, A. K and A. Prakash. 2014. Bubble column with internals: effects on hydrodynamics and local heat transfer. *Journal of chemical engineering research and design*. 92(1), 25-33.

Kalacheva, G. S., N. O. Zhila, T. G. Volova, and M. I. Fladyshev, 2002. The effect of temperature on the lipid composition of the green alga *Botryococcus*. *Journal of Microbiology*. 71, 286-293.

Kitaya, Y., H. Azuma, M. Kiyota, 2005. Effect of temperature, CO_2/O_2 concentrations and light intensity on cellular multiplication of microalgae, *Euglena gracilis*. *Journal of Advances in Space Research* 35, 1584-1588.

Korea Energy Economics Institute (KEEI). 2014. Http://www.keei.re.kr.

Kunjapur, A. M. and R. B. Eldridge, 2010. Photobioreactor design for commercial biofuel production from microalgae. *Journal of Industrial and Engineering Chemistry Research*. 49, 3516-3526.

Li, J., N. S. Xu and W. W. Su, 2003. Online estimation of stirred-tank microalgal photobioreactor cultures based on dissolved oxygen measurement. *Journal of Biochemical Engineering*. 14, 51-65.

Li, Y., W. Zhou, B. Hu, P. Chen, RR. Ruan, 2012. Effect of light intensity on algal bimass accumulation and biodiesel production for mixotrophic strains *chlorella kessleri* and *chlorella protothecoide* cultivated in highly concentrated municipal wastewater. *Journal of Biotechnol and Bioengineering*. 109(9), 2222-2229.

Luo, H. P. and Al-Dahhan, M. H. 2003. Analyzing and modeling of photobioreactors by combining first principles of physiology and hydrodynamics. *Journal of biotechnology and bioengineering*. 85(4), 382-393.

Merchuk, J. C., and Wu. X. 2003. Modeling of photobioreactors: Application to bubble column simulation. *Journal of applied phycology*. 15, 163-169.

Manual, A. U. S. 2012. Ansys Inc. Canonsburg, PA

Ministry of Trade Industry and Energy (MOTIE). 2014; 2015. Http://www.motie.go.kr

Miron, A. S., A. C. Gomez, F. G. Camacho, E. M. Grima, and Y. Chisti, 1999. Comparative evaluation of compact photobioreactors for large-scale monoculture of microalgae. *Journal of biotechnology*. 70, 249-270.

Oh, H. M and G. Y. Rhee. 1991. A comparative study of microalgae isolated from flooded rice paddies: light limited growth, C fixation, growth efficiency and relative N and P requirement. *Journal of applied phycology*. 3, 211-220.

Ohki, Y., and Inoue, H., 1970. Longitudinal mixing of the liquid phase in bubble columns. *Journal of chemical engineering science*. 25, 1-16.

Park, H, J., E. J. Jin, T. M. Jung, H. Joo, and J. H. Lee, 2010. Optimal culture conditions for photosynthetic microalgae *nanochloropsis oculata*. *Journal of applied chemical engineering*. 21, 659-663.

Peter, T and R. Anders, 2005. LDA measurements of liquid velocities in a refractive index matched packed bubble column. *Journal of chemical engineering science*. 60, 717-726.

Pruvost, J., L. Pottier, and J. Legrand, 2006. Numerical investigation of hydrodynamic and mixing conditions in a torus photobioreactor. *Journal of Chemical Engineering Science*. 61, 4476-4489.

Pulz, O., 2001. Photobioreactors: production systems for phototrophic microorganisms. *Journal of Applied Microbiology and Biotechnology*. 57, 287-293.

Qiang. H and A. Richmond. 1996. Productivity and photosynthetic efficiency of *spirulina platensis* as affected by light intensity, algal density and rate of mixing in a flat plate photobioreactor. *Journal of applied phycology*. 8, 139-145.

Rampure, M. R., A. A. Kulkarni., and V. V. Ranade. 2007. Hydrodynamics of bubble column reactors at high gas velocity: experiments and computational fluid dynamics (CFD) simulations. *Journal of industrial engineering chemical research*. 46, 8431-8447.

Rubio, F. C., A. S. Miron, M. C. C. Garcia, F. G. Camacho, E. M. Grima., and Y. Chisti, 2004. Mixing in bubble columns: a new approach for characterizing dispersion coefficients. *Journal of Chemical Engineering Science*. 59, 4367-4376.

Sato, T., Usui. S. Tsuchiya, and Y. Kondo, 2006. Invention of outdoor closed type photobioreactor for microalgae. *Journal of Energy Conversion and Management*. 47, 791–799.

Schlagermann, P., G. Gottlicher, R. Dillchneider, R. Rosello-Sastre, and C. Posten, 2012. Composition of algal oil and its potential as biofuel. *Journal of Combustion*. 2012, 1-14.

Seo, I. H., I. B. Lee, H. S. Hwang, S. W. Hong, J. P. Bitog, K. S. Kwon, C. G. Lee,

Z. H. Kim, and J. L. Cuello, 2012. Numerical investigation of a bubble-column photobioreactor design for microalgae cultivation. *Journal of Biosystems Engineering*. 113, 229-241.

Seo, I.H., 2014. Development and application of microalgal photobioreactor performance model uisng CFD. ph.D. diss., Seoul National University, Seoul, South Korea.

Seo, I. H., I. B. Lee, S. W. Hong, J. P. Bitog, K. S. Kwon, C. G. Lee, and Z. H. Kim, 2014. Evaluation of a Photobioreactor performance grafting Microalgal growth model and Particle tracking technique using CFD. *Journal of Transactions of the ASABE*. 57, 121-139.

Sierra, E., F. G. Acien, J. M. Fernandez, J. L. Farcia, C. Gonzalez, E. Molina. 2008. Characterization of a flat plate photobioreactor for the production of microalgae. *Journal of Chemical Engineering*. 138, 136-147.

Silva, H.J., Cortinas. T, and Ertola. R.J, 1987. Effect of hydrodynamic stress on *dunaliella* growth. *Journal of Chem. Technol. Biotechnol*. 40, 41–49.

Sostaric, M., J. Golob, M. Bricelj, D. Klinar, and A. Pivec, 2009. Studies on the growth of *chlorella vulgaris* in culture media with different carbon sources. *Journal of Chemical and Biochemical Engineering*. 23, 471-477.

Steele, J. H. 1977. In: microbial kinetics and dynamics in chemical reactor theory. Vol 7 (Ed. By L. Lapidus and N.R. Anunson). 405-483. Prentice-Hall, Engelwood Cliffs, NJ.

Su, Z., R. Kang, S. Shi, W. Cong, Z. Cai. 2010. Study on the destabilization mixing in the flat plate photobioreactor by means of CFD. *Journal of biomass and bioenergy*. 34, 1879-1884.

Suzuki, T., T. Matsuo, K. Ohtaguchi, and K. Koide, 1995. Gas-sparged bioreactors

for CO_2 fixation by *dunaliella tertiolecta*. *Journal of Chemical technology and Biotechnology*. 62, 351-358.

Ugwu, C. U., H. Aoyagi, and H. Uchiyama, 2008. Photobioreactors for mass cultivation of algae. *Journal of Bioresource Technology*. 99, 4021-4028.

Xu, L., P. J. Weather, X. Xiong, and C. Liu. 2009. Microalgal bioreactors: Challenges and opportunities. *Journal of Engineering in Life Sciences*. 9 (3), 178-189.

Yakubu, F, and Gumery, 2010. Mixing characteristics of draft tube airlift bioreactor using the electrical resistance tomography. Ms. diss., Ryerson University, Toronto, Canada.

Yu, G., Y, Li. Y, G. Shen, W. Wang, C. Lin, H. Wu, and Z. Chen, 2009. A novel method using CFD to optimize the inner structure parameters of flat photobioreactors. *Journal of applied phycology*. 21, 719-727.

Yeo, U. H., Y. S. Jo, K. S. Kwon, T. H. Ha, S. J. Park, R. W. Kim, S. Y. Lee, S. N. Lee, I. B. Lee, I. H. Seo, 2015. Analysis on ventilation efficiency of standard duck house using computational fluid dynamics. *Journal of the Korean society of agricultural engineers*. 57 (5), 51-60.

Zhang, D., P. Dechatiwongse, K. Hellgardt. 2015. Modelling light transmission, cyanobacterial growth kinetics and fluid dynamics in a laboratory scale multiphase photobioreactor for biological hydrogen production. *Journal of Algal research*. 8, 99-107.

Zhang, Q. H., X. Wu, S. Z. Xue, Z. H. Wang, C. H. Yan, and W. Cong, 2013. Hydrodynamic charateristics and microalgae cultivation in a novel flat-plate photobioreactor. *Journal of Biotechnology Progress*. 29 (1), 127-134.

국문 초록

광생물반응기 설계를 위한 구조변수의 통계적 분석

여 욱 현
생태조경·지역시스템공학부 지역시스템공학 전공
서울대학교 대학원

우리나라는 2014년 기준 약 95%의 높은 에너지 수입 의존도를 나타내고 있다 (KEEI, 2014). 그러나 높은 에너지 수입 의존도는 원유 수급 현황에 따라 국가 경제 및 에너지 안보를 위협할 수 있는 요인일 뿐만 아니라 대부분의 탄소화합물이 연소과정에서 CO_2로 결합됨에 따라 지구온난화로 인한 이상기후현상을 심화시킬 가능성이 농후하다. 이에 정부는 2013년 1차 에너지 대비 3.5%에 불과하던 신재생에너지의 비중을 증가시켜 2035년까지 13.4%까지 확대 계획을 고시하였다 (MOTIE, 2014).

신·재생에너지 가운데 바이오매스는 탄소 중립적이며, 전세계에서 1년간 생산되는 에너지는 전체 석유 매장량과 유사하다고 알려져 있다. 또한 바이오매스는 적절하게 이용하면 고갈의 염려가 없으며, 바이오소재의 생산도 가능하여 활용도가 매우 높다. 특히, 신·재생에너지 가운데 유일한 액체연료로써, 수송용 차량의 원료로 이용될 수 있다. 바이오매스 생산자원 중 미세조류를 이용한 바이오디젤 생산은 빠른 성장속도를 바탕으로 높은 생산성을 나타내는 미세조류의 특성에 따라 다른 생산 자원 (곡물류 및 목질류)과 비교하여 최대 1,000배 이상의 높은 효율을 가진다.

미세조류는 광합성을 기반으로 생장하는 수중 단세포 생물로써 배양과정에서 적절한 태양광, CO_2, 배양온도, 영양물질 (N, P) 등이 요구된다. 미세조류를 배양하기 위한 배양시스템은 크게 자연환경조건을 그대로 이용하는 개방형 배양시스템과 인공적으로 미세조류의 생장환경을 조절할 수 있는 폐쇄형 배양시스템으로 나뉜다. 개방형 배양시스템은 대량생산에 용이한 장점을 갖지만 광, CO_2 농도, pH 등의 환경 조절이 어려우며 오염물의 유입가능성이 크다는 단점을 가지고 있다. 반면 폐쇄형 배양시스템은 인공적인 환경조절이 가능하고, 증발로 인한 배양액의 손실 및 오염물질의 유입을 방지할 수 있다. 특히, 우리나라의 좁은 국토면적을 고려하였을 때 실효성이 높은 것으로 나타나고 있다.

광생물반응기의 대형화는 다량의 바이오디젤 자원을 확보하고 상업화하기 위하여 필수적이다. 대형화에 따른 용량 증가는 반응기 내부의 광 투과율을 감소시킴에 따라 미세조류의 생산량은 급격히 감소시킨다. 그러나 배양액의 혼합개선을 통하여 광생물반응기 내부의 미세조류가 광합성을 위하여 흡수하는 광 강도 및 이의 균일성을 향상시킴으로써 생산량을 증가시킬 수 있다. 내부의 혼합특성에 영향을 미치는 광생물반응기 내부의 구조변수는 노즐 수 및 배열, 배플 설치유무 그리고 배플 상·하부 높이 등이 있다. 이는 미세조류의 광 노출빈도, 균일성 그리고 물질교환 속도를 향상시키기 때문에 이에 대한 고려가 중요하다.

따라서, 본 연구에서는 우선 단위 모듈의 형태로 광생물반응기가 온실 내부에 설치된다는 가정하에 배양일에 따라 감소하는 광 투과깊이를 고려하여 광을 최대한 효율적으로 이용하기에 적합한 광생물반응기의 설계치수를 산정하였다. 그 후, 전산유체역학을 기반으로 BPMG (Biomass production prediction grafting mixing and growth model, BPMG) 모델을 적용하여 광생물반응기 내부의 구조변수조건에 따른 미세조류 생산량을 예측하였다. 마지막으로, 통계분석을 통하여 광생물반응기 설계에 있어서 구조변수의 우선순위와 상호작용 효과를 제공하고자 하였다.

대상 광생물반응기는 단위모듈의 형태로써, 온실 내부에 설치된다는 가정하에 배양일에 따라 감소하는 광 투과 깊이를 고려하여 설계치수가 단위 폭 (0.5m), 깊이 (0.26m), 높이 (1.7m)로 구성되었다.

광생물반응기를 설계함에 있어서 유동조절장치인 배플의 설치는 내부 혼합특성을 개선함에 따라 미세조류가 흡수하는 평균 광강도 및 광 균일성을 개선하여 생산량을 평균 40%개선됨을 확인할 수 있었다. 그러나 광생물반응기 내부에 무조건적인 배플 설치가 미세조류의 생산량에 긍정적인 효과가 있는 것이 아니며 하부높이, 설치 깊이 등의 적절한 고려가 필요할 것으로 판단되었다. 배플 설치 깊이에 따른 효과 분석 결과를 통하여 광이 투과되는 면으로부터 배플이 더 가까이 설치될수록 더 높은 미세조류의 생산량을 나타냈다. 또한 배플 하부높이에 따른 미세조류의 생산량의 경우에는 하부 높이가 증가할수록 생산량은 오히려 감소하는 경향을 보였다.

각 구조변수의 상호작용효과분석에서 배플 설치깊이 그리고 배플 하부높이에서 신뢰구간 95%에서 유의한 차이를 나타냈고 그 외 구조변수의 상호작용에서는 유의하지 않는 차이의 결과를 나타냈다. 주효과 분석결과에 대한 Bonferroni 사후검증결과에서는 설치깊이와 하부높이에서 신뢰구간 99.9%에서 유의한 차이를 나타냈다. 또한 생산량에 대한 이들의 상대적인 영향력의 크기를 분석하기 위하여 t 값을 비교한 결과 설치 깊이 (-8.437^{***}), 하부높이 (-5.346^{***}), 그리고 노즐 수 (1.975) 의 순서로 영향력이 큰 것으로 나타났다.

키워드 : 광생물반응기, 상호작용, 전산유체역학, 주효과, 혼합성능평가

Student Number : 2013-23258